**Atmospheric
Chemistry
and Physics
Discussions**

**Evaluation of
chemical transport
model predictions**

C. A. Stroud et al.

Title Page	
Abstract	Introduction
Conclusions	References
Tables	Figures
I◀	▶I
◀	▶
Back	Close
Full Screen / Esc	
Printer-friendly Version	
Interactive Discussion	

Evaluation of chemical transport model predictions of primary organic aerosol for air masses classified by particle-component-based factor analysis

C. A. Stroud[1], M. D. Moran[1], P. A. Makar[1], S. Gong[1], W. Gong[1], J. Zhang[1],
J. G. Slowik[4], J. P. D. Abbatt[4], G. Lu[1], J. R. Brook[1], C. Mihele[1], Q. Li[2], D. Sills[3],
K. B. Strawbridge[1], M. L. McGuire[4], and G. J. Evans[4]

[1]Air Quality Research, Science and Technology Branch, Environment Canada, 4905 Dufferin
Street, Toronto, M3H 5T4, ON, Canada
[2]Ontario Region Operational Forecasting, Environment Canada, 4905 Dufferin Street, Toronto,
M3H 5T4, ON, Canada

[3]Cloud Physics and Severe Weather Research, Science and Technology Branch, Environment Canada, 4905 Dufferin Street, Toronto, M3H 5T4, ON, Canada
[4]Department of Chemistry University of Toronto 80 St. George St. Toronto, M5S 3H6, ON, Canada

Correspondence to: C. A. Stroud (craigstroud@ec.gc.ca)

Evaluation of chemical transport model predictions

C. A. Stroud et al.

Title Page

Abstract	Introduction
Conclusions	References
Tables	Figures

Back | Close

Full Screen / Esc

Printer-friendly Version

Interactive Discussion

Abstract

Observations from the 2007 Border Air Quality and Meteorology Study (BAQS-Met 2007) in southern Ontario (ON), Canada, were used to evaluate Environment Canada's regional chemical transport model predictions of primary organic aerosol (POA). Environment Canada's operational numerical weather prediction model and the 2006 Canadian and 2005 US national emissions inventories were used as input to the chemical transport model (named AURAMS). Particle-component-based factor analysis was applied to aerosol mass spectrometer measurements made at one urban site (Windsor, ON) and two rural sites (Harrow and Bear Creek, ON) to derive hydrocarbon-like organic aerosol (HOA) factors. Co-located carbon monoxide (CO), $PM_{2.5}$ black carbon (BC), and PM_1 SO_4 measurements were also used for evaluation and interpretation, permitting a detailed diagnostic model evaluation.

At the urban site, good agreement was observed for the comparison of daytime campaign PM_1 POA and HOA mean values: $1.1\,\mu g\,m^{-3}$ vs. $1.2\,\mu g\,m^{-3}$, respectively. However, a POA overprediction was evident on calm nights due to an overly-stable model surface layer. Biases in model POA predictions trended from positive to negative with increasing HOA values. This trend has several possible explanations, including (1) underweighting of urban locations in particulate matter (PM) spatial surrogate fields, (2) overly-coarse model grid spacing for resolving urban-scale sources, and (3) lack of a model particle POA evaporation process during dilution of vehicular POA tail-pipe emissions to urban scales. Furthermore, a trend in POA bias was observed at the urban site as a function of the BC/HOA ratio, suggesting a possible association of POA underprediction for diesel combustion sources. For several time periods, POA overprediction was also observed for sulphate-rich plumes, suggesting that our model POA fractions for the $PM_{2.5}$ chemical speciation profiles may be too high for these point sources.

At the rural Harrow site, significant underpredictions in PM_1 POA concentration were found compared to observed HOA concentration and were associated, based

on back-trajectory analysis, with (1) transport from the Detroit/Windsor urban complex, (2) longer-range transport from the US Midwest, and (3) biomass burning. Daytime CO concentrations were significantly overpredicted at Windsor but were unbiased at Harrow. Collectively, these biases provide support for a hypothesis that combines a current underweighting of PM spatial surrogate fields for urban locations with insufficient model vertical mixing for sources close to the urban measurement sites. The magnitude of the area POA emissions sources in the US and Canadian inventories (e.g., food cooking, road and soil dust, waste disposal burning) suggests that more effort should be placed at reducing uncertainties in these sectors, especially spatial and temporal surrogates.

1 Introduction

Primary particulate-matter (PM) emissions have important health impacts on cardio-vascular morbidity and lung function (Pope and Dockery, 2006). Even trace levels of some directly-emitted aerosol chemical components (e.g., PAHs, dioxins) can be quite toxic and have significant adverse human health effects (Boström et al., 2002; Mauderly and Chow, 2008). PM emissions are also essential in determining cloud-condensation-nuclei number concentration, which impacts cloud radiative forcing properties and regional-scale climates (Zhang, 2008; Grell et al., 2011). However, it is challenging to establish a cause-and-effect relationship with specific sources contributing to PM because of the wide array of particle sources and atmospheric transformation mechanisms. To simulate the complex processing of primary PM emissions in the earth system, air quality (AQ) and climate modeling systems are being developed as predictive tools (e.g., *IPCC AR4 WG1*, 2007; Kelly et al., 2011) and for providing policy guidance for emission reduction strategies via retrospective simulations (e.g., Environment Canada and Health Canada, 2011).

The carbonaceous component of PM is the most complex component to characterize due to the wide range of constituent organic compounds with different sources and varying chemical reactivity and physical properties such as volatility, light scattering,

Title Page

Abstract | Introduction

Conclusions | References

Tables | Figures

◀ | ▶

◀ | ▶

Back | Close

Full Screen / Esc

Printer-friendly Version

Interactive Discussion

Full Screen / Esc

Printer-friendly Version

Interactive Discussion

light absorption, and hygroscopicity. Organic aerosol (OA) and black carbon (BC) are two key PM chemical components that are co-emitted from combustion sources. An organic carbon coating on BC particles can alter their morphology (Chan et al., 2010) by enhancing the collapse of BC clusters, which can in turn alter the scattering and
5 absorption properties of the emitted particles (Andreae and Gelencsér, 2006). The organic component of combustion aerosol is relatively hydrophobic, typically, >85 % by mass (Schauer et al., 1999; Sage et al., 2008). In experimental dilution samplers, the organic component of combustion aerosol has been shown to obey absorptive partitioning theory (e.g., Robinson et al., 2010), which suggests that it is dynamic in
10 nature and can evaporate on dilution to atmospheric scales.

Primary organic aerosol (POA) is defined as directly emitted organic aerosol. POA has received less attention in the literature than secondary organic aerosol (SOA). However, POA is important because it is emitted in large quantities on urban scales, it can act as a seed for vapour condensation, and it is believed to contain some toxic
15 materials. Traditionally, POA has been thought of as an inert tracer in models; however, recent laboratory studies have raised some doubts about this assumption (Robinson et al., 2010). For the above reasons, it is important to try to isolate POA from SOA in model evaluation studies.

POA is challenging to model because its emissions have large uncertainties (they
20 are not quantified directly in national emissions inventories) and the spatial surrogate fields that are used to disaggregate non-point POA emissions geographically are under continual development. Nonetheless, source-oriented AQ modeling systems have advanced in terms of predicting POA and SOA ambient concentrations and in estimating biogenic and anthropogenic contributions to SOA formation. Good agreement between
25 source-resolved models and receptor-based analysis can also increase our confidence in the source apportionment of POA.

Ying et al. (2007) used the CIT/UCD model to evaluate Los Angeles $PM_{2.5}$ data. BC and OA concentrations were underpredicted at rush-hour periods, which was attributed to a bias in the diesel emission inventory. Bhave et al. (2007) performed a

diagnostic evaluation of CMAQ-model-predicted PM$_{2.5}$ OA using molecular marker measurements from eight sites in the southeast US during the summer. Results indicate that the modelled contributions from vehicle exhaust and biomass combustion were unbiased across the region for most sites; however, in Atlanta, overestimation of vehicle emissions was significant but was partially compensated by underestimates of other sources. Lane et al. (2007) evaluated the PMCAMx model against chemical-mass-balance results from sites in the eastern US There was evidence that POA concentrations from natural gas, wood burning, and off-road diesel combustion were overestimated.

OA data acquired by the Aerosol Mass Spectrometer (AMS) instrument have been deconvolved into hydrocarbon-like OA (HOA) and oxygenated OA (OOA) components (Zhang et al., 2005a). HOA has been linked to primary emissions such as fuel combustion and has similar AMS spectra to unburned lubricating oil. Mohr et al. (2009) analyzed the unit resolution AMS spectra from meat cooking, plastic burning, paper burning, and wood burning and concluded that meat cooking and plastic burning grouped with the HOA factor, whereas paper burning and wood burning grouped on a unique factor (termed BBOA). Zhang et al. (2007) performed factor analysis on AMS data from 37 field campaigns and found that HOA represented 36 % and 17 % of OA at urban and suburban sites, respectively. A positive matrix factorization (PMF) analysis of AMS data in Zurich, Switzerland during the summer (Lanz et al., 2007) ascribed a 10 % contribution from fuel combustion and a 10–15 % contribution from local food cooking to OA in which both sources loaded onto the HOA factor with a 2-component solution (HOA, OOA) but were separated with a 3-component solution (HOA, food cooking, OOA). In Pittsburgh in the summer, HOA accounted for 34 % of OA and the OM:OC ratio was measured to be 1.2 (Zhang et al., 2005b). In Hong Kong in the summer, HOA accounted for 35 % of OA for regional air masses and 75 % for local episodes (Hu et al., 2010), while in Beijing during the summer Olympic Games, HOA accounted for 42 % of OA. In Tokyo during the summer, it has been observed that HOA does not exhibit a strong diurnal variation unlike the OOA factor (Takegawa et al., 2006).

Zhang and Ying (2010) used the UCD/CIT model to study the source contributions to PM$_{2.5}$ in the Houston-Galveston, Texas area. PM$_{2.5}$ BC in the 4-km model domain was largely from diesel combustion while POA was largely from a combination of gasoline and diesel combustion and industrial sources. Household cooking, waste disposal,
5 agricultural burning, road dust and construction were also significant contributors to POA. Predicted POA from diesel and gasoline combustion agreed well with observed HOA, but POA from biomass burning (BBOA) under-represented the biomass burning organic factor and differences were attributed to wildfire emissions missing from the inventory.
10 Other receptor-oriented models have been used to estimate POA contributions to PM$_{2.5}$. Pachon et al. (2010) compared four methods to estimate POA and SOA contributions to long-term filter measurements of PM$_{2.5}$: BC tracer; regression; carbon mass balance (CMB); and PMF. In Atlanta over several years, the CMB method gave the lowest estimate of the relative contribution of POA (54 %) and PMF gave the high-
15 est (74 %). Williams et al. (2010) performed hourly measurements of source marker species at Riverside, California during the summer and their PMF analysis showed that primary contributions to OA were 11 % from fuel combustion, 10 % from food cooking, and 7 % from forest fires. Dreyfus et al. (2009) used organic molecular composition measurements for an autumn period in Wilmington, Delaware in a PMF analysis to
20 identify six factors linked to specific sources (diesel exhaust, road dust, meat cooking) or types of compounds (alkanes/alkanoic acids, phthalates, PAHs). For the POA sources, ~1/3 was contributed from fuel combustion (largely diesel) and ~2/3 was from non-combustion sources (dust, meat cooking).

Combustion POA is semi-volatile at atmospheric dilution ratios inside dilution sam-
25 plers measuring fuel combustion (Robinson et al., 2007) and thus its gas-particle partitioning varies continuously with changing temperature and solvent mass loadings. The dynamic nature of this partitioning has important implications and adds significant uncertainty in applying current national emissions inventories (NEI), which assume non-volatile POA. The absorptive partitioning equation for organic gases (Pankow, 1994) is

Evaluation of chemical transport model predictions

C. A. Stroud et al.

Full Screen / Esc

Printer-friendly Version

Interactive Discussion

calculated by the formula

$$K_{p,i} = \frac{fRT}{10^6 \overline{MW} \varsigma_i p_{L,i}^0} \quad , \tag{1}$$

where $K_{p,i}$ is the partitioning constant (the ratio of particle mass mixing ratio to gas concentrations of the i-th compound), R is the gas constant, T is the temperature, f is the absorptive mass fraction of the PM, $\overline{MW}$ is the mean molecular mass of the absorbing phase, ς_i is the mole-fraction scale activity coefficient in the absorbing phase, and $p_{L,i}^0$ is the vapour pressure of the pure liquid. As the value of f increases (i.e., as the loading of POA increases) the partitioning will favour larger values of $K_{p,i}$ (i.e. increasing the partitioning to the condensed phase. Increases in SOA during the chemical aging of fresh emissions will also likely increase the partitioning of POA material to the particle phase, but the SOA and POA mixing state is still poorly known for atmospheric particle compositions. The high loadings inherent in the sampling protocol used to create the NEIs ($>1000\,\mu g\,m^{-3}$, 47 °C) thus suggest that the resulting POA emissions are overestimated relative to that collected in a dilution sampler at more representative atmospheric conditions ($10\,\mu g\,m^{-3}$ and 25 °C) (Robinson et al., 2010). The assumption that absorptive partitioning behavior always holds in the atmosphere is uncertain, as emitted particles mix with background pollution and other condensing gases may change the emitted particle's surface sorptive properties. Similarly, emitted semi-volatile gases mix with pre-existing inorganic particles and oxidants, which can affect how long this semi-volatile organic material remains as a gas (Liggio et al., 2005; Li et al., 2011).

The above studies suggest that significant discrepancies can exist between source-oriented models, which rely on NEIs, and receptor-based measurement-derived mass concentrations of POA. The diversity of POA sources adds further uncertainty as source intensity levels (e.g., vehicle distance traveled), fuel-based PM emission factors (e.g., mass of PM per distance traveled), PM chemical and size profiles (e.g., POA fraction of PM, PM_1 fraction of $PM_{2.5}$), source spatial and temporal profiles, as well as

organic-component volatility distribution (Robinson et al., 2010) all need to be known for each source affecting an airshed. The chemical history of the particle may also affect the partitioning via the f, $\overline{MW}$ and ς_i terms in Eq. (1).

Samaali et al. (2011) recently performed an AQ-model-based source apportionment study of primary PM$_{2.5}$ EC and POA components for cities across Canada. Four tagged source categories were considered (on-road mobile, off-road mobile and area, minor-point, and major-point sources). The on-road mobile contribution to POA was highest for Montreal, Canada at 27%. Brook et al. (2011) presented results of a model sensitivity simulation where local emissions were "zeroed out" to assess the transboundary transport of pollutants, including POA, into southwestern Ontario. Also, Meteorological Service of Canada performed a modelling assessment of the impact of biodiesel fuels on AQ indicators for Canadian airsheds (Environment Canada, 2011). All three of the above applications made use of the Environment Canada (EC) AURAMS AQ modelling system. It is thus of interest to evaluate in detail the model's POA capabilities in order to assess the performance of both AURAMS and the existing NEI's.

The Border Air Quality and Meteorology Study (BAQS-Met 2007) collected state-of-the-art, high-time-resolution OA measurements at two rural sites and one urban site in southwestern Ontario (Brook et al., 2011). Southwestern Ontario is home to some of the highest PM concentration levels in Canada. Southwestern Ontario is also one of the most challenging regions for AQ predictions due to the presence of both a wide range of sources and complex mesoscale meteorology associated with the southern Great Lakes of North America.

This study presents a detailed evaluation on the current state of chemical transport model (CTM) predictions of primary organic aerosol (POA) using Environment Canada's unified regional AQ modelling system (Makar et al., 2010a; Stroud et al., 2011), recent Canadian and US national emissions inventories, and detailed field measurements from the BAQS-Met field study.

The objectives of this study are to quantify biases that can be expected in EC's unified AQ modelling system as it is used for guiding policy decisions and to identify

where the greatest uncertainties reside so as to guide future model improvements. The specific goals are to (1) generate POA model performance statistics for the entire BAQS-Met period, (2) evaluate model POA bias as a function of POA mass concentration and other indicators of air-mass sources and history (e.g., carbon monoxide, BC, sulfate), (3) identify case study periods to diagnose systematic biases further, and (4) evaluate case-study periods to determine which source regions and PMF factors have large model errors and identify possible causes.

The paper is organized as follows. Section 2 describes the scientific methods that were used; Sect. 3 presents results with discussion on: (3.1) POA sources affecting the study area, (3.2) campaign statistics for POA at the Windsor urban site, (3.3) campaign statistics for CO and BC at Windsor, (3.4) POA time series at Windsor, (3.5) correlation plot for POA bias as a function of POA and indicator ratios, (3.6) campaign statistics for POA at the rural sites, (3.7) campaign statistics for CO and EC at the rural sites, (3.8) case studies, and (3.9) recommendations for future work. Lastly, Sect. 4 provides a summary and conclusions. A list of acronyms is provided at the end of the text.

2 Methodology

2.1 BAQS-Met field study and supersites

The BAQS-Met field campaign was conducted from 20 June to 10 July 2007 in southwestern Ontario east of the Detroit, Michigan-Windsor, Ontario urban area and close to the international border between Canada and the US The Detroit-Windsor urban area is also a major industrial area with automobile manufacturing, steel production, chemical production, electric power generation and petrochemical refining sectors. The BAQS-Met study area is also influenced by major point emission sources located along the St. Clair River (petrochemical refineries and electric-power generating stations) and other cities such as Toledo and Cleveland and electric-power generating stations located on the southern shores of Lake Erie (see Fig. 1).

The study area is also frequently impacted by long-range transport of pollution from the Ohio Valley and US Midwest into southern Ontario. In addition to synoptic-scale flows, complex mesoscale circulations frequently occur in the BAQS-Met study area in the summer due to the presence of two of eastern North America's five Great Lakes, Lakes Erie and Huron, and another large lake, Lake St. Clair. These terrain-forced mesoscale circulations, including multiple lake breezes and land breezes, can have a strong influence on pollutant transport and transformation, including the pollutants carried in the urban plume from Detroit-Windsor (Sills et al., 2011).

Four AQ super-sites were operated during the study; their locations are shown in Fig. 1. The Windsor site was located in the eastern half of that city just south of a major highway carrying cross-border traffic to the Ambassador Bridge joining Canada and the US The Bear Creek site was located ∼60 km east of Detroit-Windsor across Lake St. Clair in a wetland area surrounded by farmland. The Harrow site was ∼40 km southeast of Detroit-Windsor and ∼5 km north of Lake Erie. Harrow is also located on farmland. The Ridgetown site was the eastern-most site and was also located on farmland just north of the Lake Erie shoreline. This site geometry allowed both the Detroit-Windsor urban plume and regional air masses to be sampled simultaneously at the rural sites on many days. The high-temporal-resolution PM_1 OA data considered in this study were collected by AMS instruments at three of these sites: Windsor, Harrow, and Bear Creek. BC and CO measurements were also made at Windsor, Harrow and Bear Creek.

More information about BAQS-Met may be found in Brook et al. (2011), Hayden et al. (2011), Levy et al. (2010), Makar et al. (2010a,b), Sills et al. (2011), Slowik et al. (2011), and Stroud et al. (2011).

2.2 AQ modelling system description and setup

AURAMS is a regional AQ modelling system developed by EC; the acronym AURAMS stands for "A Unified Regional Air-quality Modelling System". AURAMS consists of three main components: a numerical weather prediction model; an off-line regional

chemical transport model (CTM); and an emissions processing system. Version 1.4.0 of the AURAMS CTM, which was used in this study, was driven by version 3.2.2 of the Canadian operational weather forecast model, GEM (Global Environmental Multi-scale model) (Côté et al., 1998) and emissions files prepared using version 2.3 of the SMOKE emissions processing system (CEP, 2011). Note that we reference specific version numbers here so that the model development and evaluation over time can be documented and accessed by the modeling community.

The GEM meteorological model with physics version 4.5 was run from 1 June to 31 August 2007 for a 575 × 641 global, variable-resolution, rotated latitude-longitude horizontal grid with a 432 × 565 uniform subgrid with 0.1375° (~15.3-km) grid spacing centered on and covering North America. 58 hybrid coordinate levels from the Earth's surface to 10 hPa were employed, with layer thickness increasing monotonically with height, and a 450-s time step was used. A high-resolution limited-area configuration of GEM was also run for part of this period (17 June to 11 July) for a domain covering the Great Lakes area: 565 × 494 x 58 grid, 0.0225° (~2.5-km) horizontal grid spacing, and 60-s time step. Output from the global GEM simulation was used to provide boundary conditions for the high-resolution limited-area GEM simulations. More details may be found in Makar et al. (2011a).

Wind fields from the high-resolution GEM simulations were also used to produce 48-hr, three-dimensional, kinematic back trajectories arriving at the BAQS-Met study super-sites (see Supplemental Information section). Back trajectories were calculated using a 120-s time step and five different arrival heights (0.05, 0.1, 0.3, 1, and 3 km) so the vertical directional shear could be estimated. The model takes into account advection by 3-D winds (Runge-Kutta temporal scheme of order 4). This trajectory model was originally developed by the Environmental Emergency Response team at EC's Canadian Meteorological Centre.

The AURAMS CTM includes representations of gas-, aqueous-, and particle-phase chemistry and predicts tropospheric ozone, size-distributed particulate matter (based on a sectional treatment), and acid deposition. Overall, the model tracks 157 species:

49 gaseous species and nine aerosol species distributed over 12 logarithmically-distributed size bins ranging from 0.01 to 41 μm in Stokes diameter. In this study, PM_1 refers to particles with a Stokes diameter less than 0.68 μm (mass in bins 1-6 and 0.042 of bin 7). This corresponds to the vacuum aerodynamic diameter particle trans-

5 mission cut-off of the AMS instrument (personal communication with Dr. John Liggio, assuming a particle density of 1.5 g/m^3 and a shape factor of unity). The nine PM chemical species considered are POA, BC, SOA, sulphate, nitrate, ammonium, crustal material (CM), sea salt, and particle-bound water. Removal processes include wet and dry deposition of both gases and particles. Operator splitting is then applied to the

10 various process parameterizations in the following order: point source emissions and plume rise; advection; vertical diffusion, gas-phase dry deposition, and surface emissions; gas-phase chemistry; aerosol processes (nucleation, condensation/evaporation, coagulation, sedimentation, dry deposition), in-cloud and below-cloud processes; and SOA formation. The most up-to-date descriptions of AURAMS process representa-

15 tions can be found in the following references: SOA formation in Slowik et al. (2010) and Stroud et al. (2011); gas-phase chemistry and speciation in Stroud et al., (2008); vertical mixing and urban-heat-island effects in Makar et al., (2006); cloud processing of pollutants in Gong et al. (2006); and aerosol particle dynamics in Gong et al. (2003).

A three-level nested grid configuration was used for the AURAMS CTM, with an outer

20 continental grid with 42-km horizontal grid spacing, an inner eastern North American grid with 15-km grid spacing, and a fine-scale 2.5-km grid over the BAQS-Met study region (Fig. 2). Twenty-eight terrain-following modified-Gal-Chen vertical layers were used with monotonically-increasing spacing to 29 km a.g.l. starting from a 15-m-thick lowest layer. The model time step was chosen proportionate to the grid spacing to

25 maintain numerical stability. For this study, a 900-s time step was used for the 42-km and 15-km simulations while a 120-s time step was used for the 2.5-km simulation. Meteorological fields were provided for the 42-km and 15-km domains from the GEM 15-km simulations and for the 2.5-km domain from the GEM 2.5-km simulations. Chemical lateral boundary conditions (CLBC) derived from climatology are assumed for the

42-km continental domain (Makar et al., 2010b). All results presented here are from the innermost, highest-resolution domain.

2.2.1 Treatment of emissions

Files of hourly, speciated, gridded anthropogenic emissions were prepared for the three
5 AURAMS CTM grids based on the 2006 Canadian, 2005 US, and 1999 Mexican NEIs using version 2.3 of the SMOKE emissions processing system. Emissions were separated into four major emissions source streams: on-road mobile (ORM) sources; off-road mobile and area (ORAA) sources; minor-point sources; and major-point sources. ORM sources include exhaust emissions and evaporative emissions from cars, light-
10 and heavy-duty trucks, buses, and motorcycles. ORAA emissions include engine emissions from construction, agricultural, commercial and residential activities, marine, rail, and air transport, coal, oil, wood, and natural gas combustion, oil sands and mining vehicle fleets, solvent use, and fugitive emissions. Point sources are larger sources that emit at least 100 tonnes (Canada) or tons (US) per year of at least one criterion
15 pollutant (i.e., SO_2, NO_x, CO, VOC, NH_3, $PM_{2.5}$, PM_{10}). Minor-point sources include chimneys and smokestacks with a stack height less than or equal to 30 m, and major-point sources include facilities with stack heights greater than 30 m (e.g., electric power generation units, smelters, refineries).

To obtain emissions of POA for the four source streams from the bulk $PM_{2.5}$ emis-
20 sions in the inventories (unspeciated emissions of particles with diameter less than 2.5 µm), four source-stream-specific $PM_{2.5}$ chemical speciation profiles were employed. The POA percentages for bulk $PM_{2.5}$were 34 % for ORM emissions, 26 % for ORAA emissions, 16 % for minor-point emissions and 16 % for major-point emissions. These splitting percentages were derived using the 2001 US NEI and PM chemical speci-
25 ation profiles from the EPA SPECIATE4.2 profile library (US EPA). The profiles were grouped into the four source streams and then each profile was mass-weighted (based on the summed emissions in the NEI that use each profile divided by the total PM in a particular source stream) to arrive at the representative averaged splitting factors for

each source stream. The speciated PM emissions thus obtained must also be size-disaggregated into the 12 size bins used by the CTM; a weighted average of measured PM size distributions for different source types was applied for each of the four source streams based on measured size distributions presented in Eldering and Cass (1996). For example, the PM_1 size fraction of $PM_{2.5}$ bulk emissions is 0.96, 0.73, and 0.99 for ORM mobile, ORAA, and point sources, respectively.

The annual inventory data were also temporally disaggregated to hourly emissions by applying source-specific monthly, weekly, and diurnal profiles within SMOKE to each of the hundreds of Canadian, US, and Mexican source types. The Canadian NEI data set was spatially disaggregated based on 42 spatial surrogate fields that, in turn, were derived from 28 socioeconomic categories in the 2001 Canadian census (e.g., population density, roadways, etc.).

Our base-case simulation assumed the POA emissions were non-evaporative. Robinson et al. (2007) published results highlighting the potential importance of POA evaporation as a diesel exhaust plume mixes in a laboratory dilution sampler. Recently, Robinson et al. (2010) suggested that, for high-emitting sources, the bias due to absorptive partitioning may be as high as ∼4 depending on the level of dilution in the atmosphere. The POA emission factors reported in Schauer et al. (1999) may also be biased high by a factor of ∼2 due to filter sampling artifacts (see Fig. 6c in Robinson et al., 2010). Over urban source regions, the modelled POA mass concentration scales close to linearly with the emissions strengths (Samaali et al., 2011). Our PM_1 POA comparison to HOA will provide further evidence to determine whether a POA evaporation hypothesis is supported in comparing our CTM predictions based on current NEI data with the ambient data.

2.3 Measurement techniques

OA measurements were made at three BAQS-Met supersites: Windsor, Harrow, and Bear Creek (see Fig. 1). The three OA measurement sites were strategically located to sample in the Detroit-Windsor air shed and the Detroit/Windsor urban plume under

common wind directions. In general, when synoptic patterns produced gradient wind flows from the southwest, Harrow received only regional background air, including the influence of the Ohio River Valley and US Midwest, whereas Bear Creek received regional background air with Detroit-Windsor emissions superimposed. Conversely,
5   when gradient wind flows were from the northwest, Bear Creek received clean continental air from northern Michigan and central Canada, whereas Harrow received this background air plus Detroit-Windsor emissions. Time periods when Bear Creek and Harrow were measuring similar POA mass concentration likely reflect periods when concentrations are representative of a regional background for the study region. In
10   practice, however, these patterns are complicated by local lake-related circulation patterns (Levy et al., 2010), so measurements need to be examined on a case-by-case basis to understand the local source-receptor relationships.

PM$_1$ OA, SO$_4$, and NO$_3$ measurements were made at both Bear Creek and Harrow using Aerodyne time-of-flight aerosol mass spectrometers (AMS), as described in de-
15   tail in Slowik et al. (2011). Briefly, particle composition was measured by a unit mass resolution instrument (C-ToF-AMS) deployed at Harrow from 17 June to 10 July and a high-resolution instrument (HR-ToF-AMS) deployed at Bear Creek from 28 June to 10 July. The AMS provides quantitative size-resolved mass spectra of the PM$_1$ non-refractory component. As described in Slowik et al. (2011), collection efficiencies for
20   both instruments were estimated on site. The OA mass spectra from the two instruments were analyzed by positive matrix factorization. The PMF solution arrived at in Slowik et al. (2011) consisted of four factors, which were labelled HOA (hydrocarbon-like OA), OOA-1 and OOA-2 (oxygenated OA, types 1 and 2), and an Unknown Factor (UNKN). The UNKN factor was a major component of OA only at the end of the study,
25   coinciding with a period of high isoprene, low aromatics, and a sulphate plume from the US Midwest.

An aerosol time-of-flight mass spectrometer (ATOFMS) was also deployed at Harrow, ON, to characterize the composition of single particles (McGuire et al., 2011). Individual particles were classified into particle-types and PMF was applied to their temporal

Evaluation of chemical transport model predictions

C. A. Stroud et al.

trends to separate into factors.

PM$_1$OA, SO$_4$, and NO$_3$ sampling with a unit-resolution AMS was also undertaken on EC's mobile laboratory, CRUISER, which was stationed for the majority of the BAQS-Met campaign in Windsor, ON. PMF analysis was also performed on the CRUISER AMS PM$_1$ data. In this case, both organic and inorganic m/z fragments were included and 6-10 factor solutions were obtained and compared to known source profiles. Given the commonality of HOA, this factor appeared in each solution and there was little difference in the profile of m/z and mass explained for the 7- to 10-factor solutions. In the 6-factor solution a biomass (wood) burning factor and the HOA factor were combined, whereas increasing the solution to seven factors separated these two factors. The 8-factor solution for HOA was selected for comparison with the AURAMS results because this HOA factor had the strongest overall correlation ($R = 0.2$) with known source profiles related to vehicle exhaust and other published HOA solutions.

The CRUISER mobile laboratory measured PM$_{2.5}$ BC at Windsor with a single particle soot photometer (SP2). At Bear Creek, EC measured PM$_{2.5}$ black carbon (BC) with a multi-angle absorption photometer (MAAP). At Harrow, the University of Toronto group measured PM$_{2.5}$ BC with a Sunset Laboratory filter-based thermo-optical instrument, and EC also measured PM$_{2.5}$ BC there with a photo-acoustic soot spectrometer (Droplet Measurement Technology). CO was measured at Windsor, Harrow and Bear Creek with an infrared spectrophotometer (Thermo Scientific TECO 48).

A scanning LIDAR instrument was deployed on the RASCAL mobile laboratory at Ridgetown. LIDAR is a remote sensing technique that provides high temporal and vertical information on atmospheric PM layers and was used to estimate daytime planetary boundary layer (PBL) mixing heights (Strawbridge, 2006). No PM composition measurements were made, however, at Ridgetown.

Meteorological measurements were made at a large number of fixed and mobile surface weather stations in the study area. Mesoscale-network measurements included wind speed and direction, dry-bulb and dew-point temperatures, pressure, and solar radiation. These surface measurements, combined with GOES-12 satellite data and

radar data from nearby US and Canadian weather radars, allowed the detection of lake-breeze circulations on each day during the intensive observation period based on mesoscale analysis. More details on the meteorological measurements and the lake-breeze detection analysis can be found in Sills et al. (2011).

3   Results and discussion

3.1   POA sources affecting the study area

Before comparing model predictions and field measurements, it is informative to study the PM emissions inventories for the Canadian province of Ontario, where the BAQS-Met field study took place, and one of the nearby upwind US states (Indiana). Tables 1 and 2 summarize annual PM_1 primary organic carbon (POC) emissions for the 2006 Ontario provincial inventory and the 2005 Indiana state inventory, respectively, where POC is the carbon-only component of POA (i.e., neglecting hydrogen, oxygen, and other constituent elements). These tabulated POC emissions were calculated by applying source-specific PM chemical speciation profiles to $PM_{2.5}$ bulk emissions from individual source types that were identified by source classification category (SCC) codes in the inventories. An additional season-specific column was added to Tables 1 and 2 to estimate 3-month summer emissions for each POA source. Seasonal scaling factors of 0.5, 0.25, or 0.0 were then applied to the annual POC mass emissions depending on the expected seasonal behaviour of the each source type to derive 3-month summer emissions. The PM_1 fraction of $PM_{2.5}$ was then applied to each source stream in the last column (see Sect. 2.2.1). Note one special case: the Indiana ORM emissions in Table 2 were present in the US NEI on a season-specific per-day basis, and thus the 3-month summer estimate was calculated by multiplication by 91 days.

For Ontario, the current NEI indicates that the ORM sector contributes (196 × 0.96) tons C/summer of PM_1 POC emissions (5 % of total) with important contributions from both diesel and gasoline engines. The off-road mobile emissions were estimated to

Title Page

Abstract	Introduction
Conclusions	References
Tables	Figures

 I◀   ▶I

◀   ▶

Back   Close

Full Screen / Esc

Printer-friendly Version

Interactive Discussion

be (1.168×0.96) tons C/summer (29 % of total) with the largest contribution coming from diesel tractors. The area sources of PM_1 POC emissions are diverse in nature and total (3.477×0.73) tons C/summer (64 % of total), with charcoal grilling (1.345×0.73), dust sources (1.208×0.73), unavailable (456×0.73), industrial metal

5 production (183×0.73) and industrial petroleum refining (111×0.73) making the largest contributions to the area sources. The minor and major point sources combined totalled (78×0.99) tons C/summer (2 % of total). The magnitudes of the POC emissions from area sources, especially from charcoal grilling, dust-related emissions, and off-road tractors, are surprising. Further investigation into the PM chemical profiles

10 (US EPA SPECIATE4.2 database) applied to calculate the $PM_{2.5}$ POC emissions from the $PM_{2.5}$ dust revealed POC percentages of 9.7 % for paved roads, 5.5 % for unpaved roads, 4.6 % for construction, and 3.1 % for agricultural. These are relatively small percentages, but when they are applied to the large $PM_{2.5}$ dust emissions from these source types they yield appreciable $PM_{2.5}$ POC emissions. Thus, the current Canadian

15 NEI and available $PM_{2.5}$ speciation profiles lead to the conclusion that area sources are the major contributor to $PM_{2.5}$ POC emissions, especially on regional scales.

For the AURAMS simulations, emissions were processed slightly differently than those for the results in Tables 1 and 2. First, source-specific $PM_{2.5}$ emissions totals were allocated spatially and temporally with SMOKE using source-type-specific spatial

20 and temporal surrogates and then were aggregated into four source streams: ORM sources; ORAA sources; and minor and major point sources. Second, the source streams for $PM_{2.5}$ were allocated chemically into five chemical components (POA, BC, SO_4, NO_3, CM) and into eight particle size bins within AURAMS. The four panels of Fig. 3 show examples of the spatial distribution of PM_1 POA emission maps for a July

25 Monday at 17:00 UTC (13:00 EST) for ORAA sources, ORM sources, and minor and major point sources. For the ORM emissions the spatial distribution is focused on major highways and urban centres, with higher emissions associated with US highways compared to Canadian highways. For the ORAA sources, the spatial distribution is much more homogeneous, with the exception of lower emissions over the lakes and to

Title Page

Abstract | Introduction

Conclusions | References

Tables | Figures

◄ | ►

◄ | ►

Back | Close

Full Screen / Esc

Printer-friendly Version

Interactive Discussion

the northeast of Bear Creek, and no large discontinuity is observed across the US and Canadian land border. The dominance of the POA area sources suggested by Tables 1 and 2 is evident in Fig. 3, with only the grid cells containing major roadways in the US and to the north of Bear Creek in the Port Huron, MI-Sarnia, ON area having ORM POA emissions greater than the ORAA POA emissions. Figure 3 also shows the POA major and minor point sources. The scales on the point-source plots are an order of magnitude larger than those used for the ORAA and ORM emissions plots. Significant point-source emissions are found in the US to the north, west, and south of the study area, but there are few POA point sources on the Canadian side of the international border and south of Bear Creek. Major point sources are often power generation stations; these have high NO_x emissions, but due to efficient combustion and to PM control technologies they are typically lower POA emitters (even though POA makes up 16 % of $PM_{2.5}$mass in our point-source profiles).

Domain totals for the entire innermost (2.5-km) modelling domain (cf. Fig. 2) show that 74 % of the PM_1 POA emissions are from ORAA sources, 12 % from major point sources, 8 % from ORM sources, and 5 % from minor point sources (see Fig. 2 and Table 3). For the entire 15-km middle nested domain, 74 % of the PM_1 POA emissions are from ORAA sources, 15 % from major point sources, 6 % from ORM sources, and 5 % from minor point sources. For the single 42 × 42 km grid cell of the outermost domain that includes Detroit and downtown Windsor, 47 % of the PM_1 POA emissions are from ORAA sources, 28 % from major point sources, 15 % from ORM sources, and 10 % from minor point sources. Thus, according to the Canadian and US NEIs, the Windsor site is strongly impacted by all emissions source streams, including ORM emissions in the Detroit/Windsor urban area and ORAA and point sources in the surrounding region. The Harrow site is impacted largely by ORAA sources, with the exception of those times when it is directly impacted by plumes from point sources or from nearby urban centers (Cleveland and Toledo along the south shore of Lake Erie and Detroit/Windsor to the northwest). At Bear Creek, ORAA and ORM sources in nearby towns and major point sources along the St. Clair River are important local sources, in addition to

Title Page

Abstract | Introduction

Conclusions | References

Tables | Figures

|◄ | ►|

◄ | ►

Back | Close

Full Screen / Esc

Printer-friendly Version

Interactive Discussion

petrochemical industries to the north in Sarnia, ON, as well as Detroit-Windsor sources to the southwest across Lake St. Clair.

Zhang et al. (2009) used monthly measurements of eight individual particle-phase organic species as well as $PM_{2.5}$ BC and OA mass over a one-year period in Detroit with PMF analysis to estimate the POA component. Three factors were derived, representing (1) urban primary sources (food cooking, road dust), (2) ORM sources, and (3) other combustion sources (coal). These three POA sources accounted for 57 % of OA mass. In Detroit, in the summer, POA concentration from ORM combustion was estimated at $0.6\,\mu g\,m^{-3}$ (60 % of POA). At a rural midwestern US site, on the other hand, the ORM-source-dominated factor was negligible compared to the other urban primary sources (food cooking, road dust) and other combustion sources (coal). The published Detroit ORM POA mass contributions are higher than those contributions summarized in Table 3.

For longer-range transport of pollutants to the study region from the southwest, the emissions in the US Midwest are of significance. This is an important synoptic flow pattern for summertime conditions in the study region (i.e., back of the Bermuda High), and gradient winds from this direction tend to be brisk (Sills et al., 2011). Table 2 shows the PM_1 POC total emissions and percent contributions for the state of Indiana, which is located southwest of the BAQS-Met study area, calculated with the 2005 US $PM_{2.5}$ NEI processed as for Table 1 with the application of SCC-specific PM chemical profiles and PM_1 fractions of $PM_{2.5}$. Note that the population of Indiana in 2005 was about half that of Ontario: 6.3 vs. 12.1 million.

ORM diesel and gasoline combustion emissions in Table 2 are comparable in magnitude and total (204×0.96) tons POC/summer (7 % of total). Off-road mobile emissions total (572×0.96) tons POC/summer (19 % of total) and are dominated by emissions from diesel tractors, gasoline pleasure craft, gasoline recreational vehicles, and gasoline lawn and garden equipment. Residential wood combustion is large in winter but would not be expected to be significant in summer. Area emissions sources total (1.863×0.73) tons POC/summer (48 % of total) and are composed

largely of dust sources, charcoal grilling, waste disposal, and coal and oil combustion for area industrial processes. Point-source emissions can be split into (498 × 0.99) tons POC/summer from industrial processes and (268 × 0.99) tons POC/summer from electricity generation, largely from coal, for a sum of (765 × 0.99) tons POC/summer (26 % of total).

Interestingly, in comparing the PM_1 POC Ontario and Indiana inventory, the sum of the on-road and off-road mobile source percentages are very similar: 34 % for Ontario and 26 % of Indiana. Ontario has higher area-source percentages than Indiana (64 % compared to 48 %) and Indiana has higher point source percentages than Ontario (26 % compared to 2 %). This is reasonable given the larger population and land area of Ontario and larger POA emissions from point sources in the US Midwest and Ohio Valley compared to Ontario, where coal-fired power generation is much less important. The Indiana inventory does give a picture of which POA area sources and point sources are estimated to be important (i.e., according to the US NEI) in terms of contributing to long-range transport of POA into southwestern Ontario. Charcoal grilling and dust are the two largest POA sources in Indiana. Industrial point sources are diverse and also very important; major emitters include oil-based boilers, metal production, fibreglass production, and coatings production among many other source types. Power-generation point sources are also more important than in Ontario. ORM sources, on the other hand, are non-negligible but weaker for the midwestern United States, including Indiana.

Table 3 also lists the emissions contributions by source stream for two related carbonaceous species, CO and $PM_{2.5}$ BC. For CO emissions in the Detroit/Windsor airshed, ORM sources and ORAA sources are comparable in magnitude while point sources make only a small contribution. For BC emissions in the Detroit/Windsor airshed, ORM sources are the dominant source followed by ORAA sources. Point sources are smaller but non-negligible. Collectively, Table 3 illustrates that POA, CO, and BC have different source signatures. In comparing these species, we cannot assume they have common sources, but they still may provide complementary information on which

sources and/or processes result in model concentration biases.

3.2 Campaign statistics for PM$_1$ POA and HOA at Windsor

Comparing model-derived POA with measurement-derived HOA must be done carefully and with the knowledge that HOA and POA are not identical quantities under all situations. HOA is derived from hydrocarbon-like fragments in the AMS, which are often strongly tied to fossil-fuel combustion but which can also be related to early-generation products of long-carbon-chain precursors (e.g., sesquiterpenes, long-chain alkanes) that become oxidized but retain hydrocarbon character. Similarly, model POA may also contain some emitted oxygenated organic species that could load onto the OOA factors. As shown in Sec. 3.1, the POA emissions inventory also contains a large fraction of OA bound to dust and it is uncertain as to whether the HOA measurement would capture this source. Given these caveats, there is uncertainty in the POA-HOA comparison but the PMF HOA factor is currently the best measurement-derived quantity to compare with model POA.

Table 4 presents the modelled PM$_1$ POA performance statistics for the urban Windsor site (see Fig. 1). Statistics are separated into three diurnal periods: daytime (09:00–14:00 EST); nighttime (18:00–06:00 EST); and rush-hour periods (06:00–09:00 and 14:00–18:00 EST). The daytime model PM$_1$ POA mean is $1.1 \pm 0.9\,\mu g\,m^{-3}$ and compares well with the measured PMF HOA factor of $1.2 \pm 1.0\,\mu g\,m^{-3}$; however, the model vs. measurement correlation yields a slope of 0.39, a model y-intercept of $0.65\,\mu g\,m^{-3}$ and a correlation coefficient, R, of 0.43. The poor correlation likely reflects possible compensating errors in the emissions inventory or a poor model timing of meteorological factors such as frontal passages, boundary-layer stability, and the exact placement of plumes. Given the selection of only daytime data, though, uncertainties in modelled near-surface vertical mixing should be reduced compared to other times. As shown in Table 3 for the Detroit/Windsor 42×42 km grid cell, it is expected that all emissions streams are important, so this good level of agreement is encouraging but we must be cautious of compensating errors.

The nighttime model mean is $2.1 \pm 2.8 \, \mu g \, m^{-3}$ with a large standard deviation compared to the measurement mean of $1.0 \pm 1.0 \, \mu g \, m^{-3}$. The large standard deviation of the model mean likely reflects uncertainties in modelling the nighttime meteorology, especially vertical mixing near the surface, while the positive bias suggests that the model's surface layer may be too stable at night or that nighttime emissions may be too large. Figure 4 presents the PM_1 POA percentage error for 15-min averaged data points at Windsor plotted against wind speed for nighttime data only. The colour coding is the ratio of the model to measured surface temperature. At night, the largest overpredictions occurred under light wind conditions (less than $1 \, m \, s^{-1}$) when the model was significantly underpredicting surface temperature (blue points), resulting in a model surface layer that was too stable compared to ambient conditions.

The rush-hour model mean POA is $1.6 \pm 1.6 \, \mu g \, m^{-3}$, which compares favourably with the HOA factor of $1.4 \pm 2.1 \, \mu g \, m^{-3}$. The HOA solution is largest at rush-hour periods compared to other times of the day. The large standard deviation on the measured mean value likely reflects both meteorological variations associated with the vertical mixing in the boundary layer and the greater variability of ORM emissions at this time associated with traffic flow patterns. The y-intercept of the model vs. measurement best-fit line is particularly large at $1.4 \pm 0.1 \, \mu g \, m^{-3}$. The slope of 0.16 ± 0.05 and correlation, $R = 0.20$, are also poor. This variability reflected in the low R value could stem from the poor spatial allocation of Canadian ORM emissions by the SMOKE program due to the use of a single spatial surrogate based on a combination of road-network and population distributions, which in hindsight over-weighted by population distribution and under-weighted roadway locations for Ontario and other provinces (see Fig. 3). A more detailed approach that employed six spatial surrogates, three for urban areas and three for rural areas, was used for spatial allocation of the US ORM emissions (Zhang et al., 2010).

Title Page

Abstract | Introduction

Conclusions | References

Tables | Figures

◄ | ►►

◄ | ►

Back | Close

Full Screen / Esc

Printer-friendly Version

Interactive Discussion

3.3 Campaign statistics for CO and PM$_{2.5}$ BC at Windsor

The model performance for two other carbonaceous species, CO and BC, may provide additional information on how well the model is performing in terms of meteorology, and ratios of POA concentration to concentrations of other carbonaceous emitted species may be less sensitive to dilution than the concentrations themselves. CO and BC, however, are unique species with their own modelling challenges. CO is not simply a long-lived passive tracer of combustion, since it is produced as a secondary pollutant from both biogenic and anthropogenic VOCs. BC is also long lived and can be influenced by upwind boundary conditions. BC is more problematic to measure, and three different techniques have been used at the three super-sites. BC sources can also differ from POA sources (e.g., diesel, fuel oil, and aircraft exhaust emissions are higher in BC than POA; see Fig. 2 in Robinson et al., 2010).

Tables 5 and 6 present the model evaluation statistics at the urban Windsor site for CO and PM$_{2.5}$ BC, respectively. During the day, the campaign-mean model CO was calculated from 15-min-average data points. The daytime model CO is significantly overpredicted with a normalized mean bias (NMB) of 134 %, a root mean square error (RMSE) of 520 ppbv, and a correlation coefficient of $R = 0.24$. Conversely, during the day, the campaign-mean model PM$_{2.5}$ BC, also calculated from 15-min-average data points, was underpredicted, with a NMB of -48 %, a RMSE of 1.4 µg m^{-3}, and a correlation coefficient of $R = 0.42$. Clearly, the three carbonaceous species (POA, CO, and BC) have considerably different biases, errors, and correlations. The NMB value of POA is considerably better than the NMB values of CO and BC during the daytime hours at Windsor: 15 % vs. 134 % and -48 %.

For the nighttime period, on the other hand, the NMB of POA increased to the same level as that for CO (100 % vs. 99 %), while the NMB for BC remained similar to its daytime value (-41 % vs. -48 %). The correlation coefficient was also very similar for all three species at night ($R = 0.41$, 0.43, and 0.43).

For the rush-hour periods, the campaign-mean model POA was unbiased

Title Page

Abstract | Introduction

Conclusions | References

Tables | Figures

◀ | ▶

◀ | ▶

Back | Close

Full Screen / Esc

Printer-friendly Version

Interactive Discussion

(NMB = 1 %), but model CO was again overpredicted (NMB = 121 %). Model PM$_{2.5}$ BC performance was improved compared to other times of day with a NMB of −30 % and a correlation of $R = 0.64$. In looking at the measurements, there was less variation between day, night, and rush-hour times for all three species than there was for
5 the model predictions. The campaign-mean model POA was highest at night while the measurements were highest during rush-hour. The campaign-mean model CO was highest at rush-hour, consistent with the measurements. The campaign-mean model PM$_{2.5}$ BC was highest at rush-hour, whereas measurement averages were very similar for all three periods.
10 Given the complexity of these trends, interpreting ratios of POA to CO or POA to BC is problematic at Windsor due to the potential for different emissions sources, mixing times, chemical lifetimes, and removal processes. The y-intercepts (model values) in the POA model-measurement scatter plots are all positive and large compared to mean modelled values. This could result from numerous possible causes, including (1) not
15 enough vertical mixing in the model in locations where there are high emissions, (2) too slow model deposition processes for urban land use, and/or (3) overly uniform spatial allocation of emissions in urban areas compared to actual emissions patterns (e.g., roads vs. human population vs. commercial surrogates).
Overall, vertical mixing appears to be a critical model process impacting the results
20 at the urban site. It is likely that the emissions inventory for CO is better characterized than POA or BC, given that CO is more easily measured and chemically and physically stable on the time scale of vertical mixing. If we assume our CO emissions are accurate, then the results may imply that urban-scale vertical mixing is underpredicted in the model. The ORAA sources are largest for CO and POA in the Detroit/Windsor
25 airshed (Table 3) and are relatively uniform over urban areas in the model (Fig. 3). This hypothesis would lead to the conclusion that urban POA emissions from ORAA sources may be underpredicted (possibly due to limitations in the spatial surrogates that were used). BC is underpredicted already, but its emissions are largely from ORM sources that may have a different emission bias and/or different mixing scales. On the

Full Screen / Esc

Printer-friendly Version

Interactive Discussion

other hand, CO emissions may have significant inaccuracies that need further improvement. ORM emissions of CO are almost as large as ORAA emissions of CO. As noted in Sect. 3.2, if the spatial surrogate field used to allocate CO emissions from ORM sources over-allocates these emissions to urban areas, then even if the magnitude of CO emissions is known accurately at the domain or subdomain level and vertical mixing is well represented, CO concentrations will be overpredicted. The same argument would apply to PM_1 POA emissions, but only 15 % of these emissions come from ORM sources for the Detroit/Windsor airshed vs. 47 % of CO emissions (Table 3).

3.4 PM_1 POA and HOA time series for Windsor

Figure 5a illustrates the observed HOA and AURAMS PM_1 POA time series for the urban Windsor site. Overall, the model captures the multi-day variations associated with synoptic-scale changes in meteorology (e.g., minimum on 3 July). The model also captures some of the early-morning maxima (e.g., maxima on 25 and 30 June). Figure 6 illustrates the model time series for PM_1 POA, PM_1 SO_4, $PM_{2.5}$ BC, and CO and measurement-derived PM_1 HOA, PM_1 SO_4, $PM_{2.5}$ BC, and CO at Windsor from 3 July to midday 5 July 2007. The time period from 3 July, 01:00–07:00 EST is of particular interest. Model POA, SO_4, and CO all increased during the first two hours; however, measurement-derived HOA, SO_4 and CO decreased in concentration. Interestingly, measured BC increased slowly and was predicted well (uncharacteristic, given that BC is typically biased low). The predicted surface temp was 5 °C lower than measured on this night and modelled wind speeds were low and from the east. This analysis suggests the modelled surface layer was too stable and local Windsor POA emissions contributed to the maximum concentration.

The early morning period on 4 July was predicted well for POA. Concentrations were moderately high in HOA and SO_4. An analysis of AURAMS surface distributions (not shown) suggested the SO_4 was of regional origin from the southwest with no distinct local plumes impacting the study sites. The model POA, BC and CO correlated in time with a large dynamic range in concentrations. Model POA did correlate with SO_4

5965

from 00:00–06:00 EST, but not with the same dynamic range as POA, BC and CO. The SO_4 change was a slower, more regional accumulation on this morning (00:00–06:00 EST). There is considerable variability in the measured HOA data, but model bias was improved. Measured CO remained constant throughout the morning suggesting
5 the measured POA change was not likely from mobile combustion sources, but rather from upwind, regionally mixed area and point sources.

Another period of interest on Fig. 6 is from July 5, 00:00-5:00 EST when model POA and model SO_4 were correlated in time and significantly overpredicted vs. measurements. Model CO and BC also increased during this time and were overpredicted, but
10 not to the same extent as POA and SO_4. Winds were also very light on this night and were from the west, and the model underpredicted the surface temperature. When the winds were from the west, the site was influenced by local point sources across the Detroit River. A little later, modelled BC and CO also have maxima at 06:00–08:00 EST, model SO_4 decreased, but for this later morning period, modelled agreement for all
15 species was variable in correlation but better in bias. Winds were more from the northwest. The high BC and CO concentrations suggest mobile sources from the urban core of Detroit were important from 06:00–8:00 EST. Overall, Fig. 6 suggests that model mixing at night is a critical modelled parameter and that model POA was high in concentration within a local model SO_4 plume under stable conditions (5 July). At this time,
20 however, the modelled SO_4 plume was not captured in the SO_4 measurements, so a more definitive statement cannot be made about the accuracy of the POA emission factor from this point source region.

Figure 7 shows time series for the same set of model and measurement species at Windsor from 8 July to midday 10 July 2007. Over this 2.5-day period, the model POA and model SO_4 correlated closely while the measured HOA and measured SO_4 did not.
25 The early morning period on 8 July (00:00–06:00 EST) showed good model and measurement agreement for SO_4 in concentration and a very strong correlation between model SO_4 and model POA, whereas measured SO_4 and HOA showed no correlation: HOA concentration remained low and steady whereas measured SO_4 increased with

time. In Fig. 7b, the model BC follows the measured BC concentration time variations for the same period but is underpredicted in magnitude, similar to the overall campaign bias. In Fig. 7c, the CO model time series is overpredicted during the early morning period on 8 July and the correlation with the CO measurements is poor. Wind speeds were relatively high from the southwest during the early morning on 8 July. AURAMS surface distributions (not shown) showed influence from local sources along the Detroit River for POA, BC, CO and SO$_4$.

During the early morning period on 10 July (05:00–08:00 EST), the model POA and SO$_4$ showed a large maximum at a coincident time (06:00 EST) while measured HOA showed no change and the measured SO$_4$ showed a smaller local maximum on a higher background. For the measured maxima in SO$_4$ on 10 July at 12:00 EST, there was no coincident increase in HOA. Winds were very light from the southwest at this time. The measured BC time series correlated with HOA, but not with measured SO$_4$; however, model BC, POA and SO$_4$ all correlated in time. Model BC underpredicted measured BC, by amounts similar to the campaign NMB. Measured and modelled CO showed little correlation in time. For the period (08:00-10:00 EST) when measured and model CO were high in concentration and agreed well, the modelled POA and measured HOA also agreed quite well. The time of the measured CO maximum was on the long tail of the model CO peak. For 10 July at 06:00 EST, the model CO maximum is at the same time as the model SO$_4$ maximum; however, the measured CO maximum was not coincident with the time of the measured SO$_4$ maximum. The measured CO maximum does not appear to be a sulphate plume but rather a gasoline combustion source during the morning rush-hour. Most importantly, the high measured SO$_4$ ($\sim$14 µg m^{-3}) at 12:00 EST does not correlate with high HOA. At 12:00 EST, the AURAMS surface distribution plot (not shown) displays high SO$_4$ channelling all along the Detroit River from the southwest. Overall, Fig. 7 provides additional evidence to Fig. 6 that modelled POA is overestimated in the modelled sulphate plumes originating from southern Detroit sources, but compares better to HOA when the model is able to capture the CO plume from local gasoline combustion-related sources.

5967

3.5 Modelled POA Bias and its correlation with indicator ratios for Windsor

Figure 8a illustrates the ratio of PM_1 POA to HOA plotted against the ratio of PM_1 model SO_4 to measured SO_4 colour-coded as a function of model SO_4 concentration at Windsor. Figure 8a indicates that points (1) close to a model SO_4 to measured SO_4
5 ratio of unity (±0.5 from unity are plotted) and (2) high in model SO_4 (e.g., point source plumes) have a ratio of POA:HOA of 10 or higher. This provides further evidence of a model tendency to predict high POA levels in SO_4 plumes. For other points with similar ratios of model to measured SO_4 close to unity but low model SO_4 concentrations (red points), the POA to HOA ratio is quite variable (unbiased to an underprediction of HOA)
10 and other sources and processes likely play more important roles.

Figure 8b shows a scatter plot of the modelled POA to HOA ratio vs. the HOA factor mass concentration for Windsor. There is an apparent trend in bias with measured mass concentration. At intermediate HOA levels, the model is unbiased; however, it underpredicts at high HOA levels and overpredicts at low HOA levels. This trend could
15 result from issues in the spatial resolution of the model grid at urban scales or from inadequacies with the spatial surrogate fields for ORM and/or ORAA sources in Windsor. This trend, however, is also consistent with the evaporation hypothesis proposed by Robinson et al. (2007) for combustion sources that have undergone significant ambient dilution. At low HOA loading, the model POA evaporation process may be needed
20 to reduce the model over-prediction at Windsor.

Figure 8c shows a scatter plot of the ratio of $PM_{2.5}$ model BC to model POA vs. the ratio of measured $PM_{2.5}$ BC to HOA and colour-coded with the ratio of model PM_1 POA to HOA (yellow is unbiased, red indicates an HOA underprediction, and blue indicates an HOA overprediction). The ratio of BC to HOA is a measure of the importance of
25 diesel and oil combustion sources relative to other sources (e.g., food cooking, soil dust, and coal and wood combustion) since BC is produced predominantly from diesel and oil combustion sources (e.g., Samaali et al., 2011). For ratios that are low in both model BC:POA and measured BC:HOA (area sources such as soil dust and meat

Title Page

Abstract	Introduction
Conclusions	References
Tables	Figures

◄◄   ►►

◄   ►

Back   Close

Full Screen / Esc

Printer-friendly Version

Interactive Discussion

cooking), these points have high ratios of POA to HOA (i.e., POA overpredictions, denoted by blue colours). This is consistent with the hypothesis that the spatial surrogates for these source types are too uniform and may need more structure at urban scales. Conversely, ratios of model and measured BC/POA that are both large (ORM and

5 ORAA sources of diesel and oil combustion) are colour-coded red, indicating underpredictions in POA. This is consistent with the Ying et al. (2007) study that concluded BC and POA levels were underpredicted in Los Angeles due to low diesel emissions in the California emissions inventory.

3.6 Campaign statistics for PM$_1$ POA and HOA at Harrow and Bear Creek

10 Table 7 summarizes the model POA performance statistics for the rural Harrow and Bear Creek sites. The daytime model mean at Harrow is $0.3 \pm 0.2\,\mu g\,m^{-3}$ compared to a PMF HOA factor of $0.8 \pm 0.7\,\mu g\,m^{-3}$. Unlike the urban site, the nighttime averages in the model and measurements are similar to the daytime averages. The averages are within the one standard-deviation of each other. However, the daytime NMB at

15 Harrow is larger than at Windsor whereas the nighttime NMB is smaller (-62% vs. 15 % in day; -51% vs. 100 % at night). Given the rural location of Harrow and its proximity to few ORM emission sources, the variability in the modelled 15-min average may be associated with pollution transport patterns to the site or emissions spatial disaggregation, both of which have large uncertainties. The campaign-averaged POA

20 under-prediction may be a result of biases in the ORAA inventory or difficulties with the model consistently representing the transport pathways of pollutants to Harrow. The model POA y-intercepts, slope, and correlation are also poor. In the summer Harrow is often impacted by lake-breeze fronts, which are difficult to model accurately both spatially and temporally (Levy et al., 2010; Makar et al., 2010a).

25 Figure 5b shows time series of measured PM$_1$ HOA and AURAMS PM$_1$ POA for Harrow. Overall, the model does not capture the magnitude of the largest HOA maxima, whereas the lowest background concentrations are captured reasonably well by the model. HOA is underpredicted on the early mornings of 20, 21, 24, 30 June and 2, 3,

and 6–9 July. The model POA is also underpredicted for a number of daytime periods at Harrow: 21, 24, 30 June and 6–9 July. Only on 28 June does the model POA consistently overestimate the HOA factor at Harrow.

Interestingly, the Bear Creek POA model mean is similar to Harrow's while the Bear Creek measured POA mean is much smaller than Harrow's. Like Harrow there is little difference between daytime and nighttime measured averages at Bear Creek, but the Bear Creek daytime model y-intercept, slope, NMB, and correlation values are much better than the corresponding values for Harrow. This may be a reflection of Bear Creek being influenced by fewer and different sources than Windsor and Harrow during the study. The dominant wind direction during the 3-week study was from the northwest (Sills et al., 2011), and this direction has few upwind point and urban sources. On the other hand, relative to Bear Creek, Harrow is downwind of the Detroit/Windsor urban area for northwesterly flow. In addition, the location of Bear Creek is such that for any wind from NW to SW quadrant, the location will be impacted by emissions from the US NEI which is arguably better characterized than the Canadian NEI, especially in the application of spatial surrogates since US emissions are reported at the county level, which is a much finer spatial scale than the Canadian emissions, which are reported at the much larger provincial level and hence are much more sensitive to the suitability and representativeness of the spatial surrogates. The transport pathways may also be better represented in the model at Bear Creek. The correlation does worsen at night for Bear Creek, but the model remains unbiased there. This may be a reflection of predicting the stability of the nocturnal boundary layer and the drainage flow of plumes from local sources along the St. Clair River.

Figure 5c shows time series of measured PM_1 HOA and AURAMS PM_1 POA for Bear Creek. AURAMS still underpredicts some of the HOA maxima, but the level of agreement can be considered good, especially for the 4–9 July period. Some of the daytime variations are captured quite well by the model (e.g., 5, 9 July).

Title Page

Abstract | Introduction

Conclusions | References

Tables | Figures

◄ | ►

◄ | ►

Back | Close

Full Screen / Esc

Printer-friendly Version

Interactive Discussion

3.7 Campaign statistics for PM$_{2.5}$ BC and CO at Harrow and Bear Creek

Tables 8 and 9 list campaign-period performance statistics for CO and PM$_{2.5}$ BC at Harrow and Bear Creek (cf. Tables 5 and 6 for Windsor). CO was largely unbiased at both sites for both daytime and nighttime periods. The correlation coefficient, R, for CO is significantly improved for these two rural sites compared to the urban Windsor site. The good agreement for CO at these two rural sites suggests that long-range transport and boundary conditions are not the cause of the poor CO model results at Windsor. This reduces the number of possible sources of model CO overprediction at Windsor, but still leaves spatial and temporal allocation of emissions and/or vertical mixing of emissions as possible explanations.

At Harrow, BC was underpredicted to a similar degree as POA (NMB = −73 % during day and −67 % at night vs. −62 % and −51 %). At Bear Creek, BC was also significantly underpredicted(NMB= −71 % during day and −67 % at night but the daytime correlation for BC at Bear Creek was the best of all three species for the three sites ($R = 0.72$). In fact, BC was consistently and significantly underpredicted at Windsor, Bear Creek, and Harrow, suggesting a problem with the magnitude of the emissions. Interestingly, at Harrow none of the three carbonaceous species display significant differences between day and night. The behaviour of POA and CO is quite different in the statistics at Harrow, while POA and BC have similar statistics in terms of NMB and correlation.

Calculations of measured and model sulphate for the entire period at Harrow showed only a small NMB of 14 %. The model and measured means were 3.3 μg m^{-3} and 2.8 μg m^{-3}, respectively. Figure 9 shows a scatter plot for model and measured PM$_1$ SO$_4$ at Harrow colour-coded as a function of the ratio of PM$_1$ POA to HOA. Points with model POA to HOA ratios greater than 1.5 tend to fall on or above the model and measurement SO$_4$ 1:1 line. This suggests that for some model SO$_4$ plumes, the POA is overpredicted (e.g. 26 June, 12:00–13:00 EST). This likely reflects the CTM's ability to predict the placement and vertical mixing of point source plumes. An examination of the AURAMS surface SO$_4$ and POA distribution on 26 June suggests Harrow was

influenced from longer range transport of plumes from point sources along the southern shore of Lake Erie. Interestingly, there are also some points close to the PM_1SO_4 model vs. measurement 1:1 line which are high in POA to HOA ratio (e.g. 17 June, 13:00–14:00 EST). This suggests that the point source PM chemical speciation profile may overweight the POA fraction for sources impacting Harrow. An examination of the AURAMS surface SO_4 and POA distribution suggests Harrow was influenced from point sources along the Detroit River on June 17; however, the model fields also suggest significant convective activity and showers on this day and this complicates further analysis.

Overall, the comparison of model POA at Harrow with HOA requires further diagnostic analysis (see next section on case studies). The fact that CO is much better predicted at the two rural sites whereas POA is often underpredicted at Harrow does support the hypothesis presented earlier that too weak vertical mixing at the urban site may result in CO overpredictions there. The air masses impacting Harrow have more time for vertical mixing out of the lowest model layer and thus are not as sensitive to mixing as at the urban Windsor site. By contrast, POA may be underpredicted at Harrow due to insufficient upwind urban emissions.

3.8 Case studies

In this section, we examine four types of case studies and eight cases to better understand the sources of model POA bias under different daytime meteorological conditions, especially the times for POA underprediction at Harrow. Case study periods were identified based on analysis of meteorological back trajectories for Harrow and Bear Creek, and, for Harrow, the single-particle component-based factor analysis results from McGuire et al. (2011). The mesoscale analysis and high-resolution back trajectories are included in the Supplement Information (SI) section. The spatial distributions of the model vertical wind speed at 390 m are also included in the SI for one case to compare with the positions of the lake-breeze fronts on the mesoscale analysis. Note that 4 July 2007 was removed as a potential case-study day due to too much

model convective instability compared to radar. A model mesoscale circulation swept through the Bear Creek region which was not observed in the winds at the mesonet sites. 30 June was also removed due to different wind directions observed and modelled near Bear Creek. At times, the position of the Lake Erie lake-breeze front was misplaced by the model (e.g., 6 July), which is important in determining which air masses were sampled at Harrow. A detailed discussion of meteorological impacts on air quality is beyond the scope of this paper. Case studies are only presented in detail here for periods when the model was felt to represent the transport accurately from a comparison with the mesoscale analysis. Sulphate will be used for further diagnosis in the case studies.

3.8.1 Detroit/Windsor urban-influenced air masses arriving at Harrow and Bear Creek

Table 10 lists the two representative case-study (CS) periods for Detroit/Windsor urban-influenced air masses arriving at Harrow (June 21) and Bear Creek (8 July). At Harrow, this corresponds to the "Organic" factor period identified in McGuire et al. (2011). Single-particle ATOFMS PMF analysis identified the likely source of the organics as fuel combustion. The "Organic" factor also correlated well with gas-phase NO_2 and $PM_{2.5}$ BC, which are both fuel combustion tracers. Examination of the measured particle size distribution for this factor revealed geometric mean diameters in the range 0.55–0.58 μm, which together suggests the "Organic" factor may be related to secondary organic aerosol. The aerosol mass spectra indicated oxidized organic species and a fragmentation pattern consistent with aromatic molecular groups. Thus, the smaller Aitken-mode HOA particles likely originated from sources that were also rich in SOA precursor gases. At Harrow, the AMS HOA factor was 17 % of the AMS OA measured mass concentration. The HOA factor ($1.4 \, \mu g \, m^{-3}$; Table 10) was also larger than the 23-day daytime average ($0.8 \, \mu g \, m^{-3}$; Table 7). Back trajectories on 21 June were also consistent with moderate NNW gradient winds and air parcels passing over southern Detroit before reaching Harrow (Section SI, CS 1a). The NMB value for POA was

Title Page

Abstract | Introduction

Conclusions | References

Tables | Figures

|◄ | ►|

◄ | ►

Back | Close

Full Screen / Esc

Printer-friendly Version

Interactive Discussion

−81 %. The AURAMS POA surface distribution map (Fig. 10) shows the Harrow site on 21 June (10:00 EST) being impacted by an electric-power generation station plume (Trenton) but little else. From the AURAMS POA surface distribution, the modelled downtown Detroit plume from the highest density of ORM emissions passed well north

5 of Harrow. The mesoscale analysis shows that measured wind directions at Harrow and nearby sites were consistent with the model winds, and the PBL heights derived from model vertical profiles were consistent with the Ridgetown LIDAR measurements.

For other species, the model and measured PM_1 SO_4 were 1.9 and 1.3 $\mu g\,m^{-3}$, respectively, over the 5-h daytime period, markedly lower than the model and measured

10 campaign means for Harrow of 3.3 and 2.8 $\mu g\,m^{-3}$. There was a short-lived maximum in the modelled SO_4 when the Trenton plume passed over Harrow ($\sim$30 min duration): however, the remaining 4.5-h period saw relatively low and constant SO_4 levels in both model and measurements. The NMB for CO was low at −17 % but the NMB for BC was −84 %, similar to that for POA (NMB = −81 %). The source region in southern Detroit

15 is heavily industrialized. The predominant wind direction in the region for the campaign was from the west to north-west (Sills et al., 2011). Given this prevailing wind sector, this case provides further evidence for a common synoptic pattern contributing to the campaign-mean negative POA bias at Harrow.

At Bear Creek on the afternoon of 8 July, the HOA factor was also larger than av-

20 erage (1.0 vs. 0.3 $\mu g\,m^{-3}$), winds were moderate from the SW and back trajectories showed air passing over industrial southern Detroit and Windsor before reaching Bear Creek (see SI, CS 1b). The modelled mean POA concentration for the 4-h period on 8 July was similar to the 23-day average (0.32 vs. 0.24 $\mu g\,m^{-3}$) and the model POA NMB was −67 %. The AURAMS POA distribution map (Fig. 10) for 8 July (13:00 EST)

25 does not show a well-defined plume being transported from southern Detroit/Windsor. The model vertical cross section parallel to the surface wind direction at Bear Creek clearly showed some surface downtown Detroit urban emissions and their vertical mixing (Fig. 10). The model mixed layer was well developed at Bear Creek by the afternoon and vertical mixing was diluting the downwind plume. The Ridgetown LIDAR

measurements were not available at this time; however, the model-derived PBL height was similar to the campaign-mean afternoon LIDAR PBL height of 1600 m. The measured HOA was consistently higher than the campaign-mean value for more than four hours, suggesting the measurements were not due to a passing localized plume. The NMB values for CO and BC of −21 % and −71 %, respectively, were similar to the above Harrow case. The similar NMB values for BC and POA may suggest a common cause for the underpredictions (e.g., area-source spatial disaggregation for urban areas, emissions activity levels for urban diesel sources). The good agreement for CO may suggest that vertical mixing issues at the urban site may lose their impact at the rural sites due to the longer transport times for mixing to take place (Tables 5 vs. Tables 8).

It is interesting that the campaign-mean daytime model bias for POA is small at the Windsor urban location, but the 21 June and 8 July cases both show a significant model POA underprediction when the Detroit/Windsor plume is impacting one of the rural sites. The mesoscale analyses for both cases suggest the model is representing the meteorology reasonably well (see SI, CS 1ab), and the wind fields are straightforward for both days, which suggest the POA emissions were more likely under-represented than dispersion was over-represented, especially from the heavily industrialized southern Detroit source region compared to the more ORM-dominated site in Windsor. Another possibility is that the oxidation of intermediate volatile organic compounds (IVOCs: e.g., long-chain alkanes) may be occurring during transport to the rural sites and weakly oxidized early-generation IVOC products may be condensing and classified as HOA in the PMF analysis. Evidence for HOA factor mass generated from the oxidation of crude oil evaporative IVOC emissions in the Gulf of Mexico (e.g., long-chain alkanes) was recently found by de Gouw et al. (2011).

3.8.2 Transport from the southwest

It was observed that several periods of transport to the region from the southwest also resulted in negative POA biases at the rural supersites. Table 11 lists the two

Evaluation of chemical transport model predictions

C. A. Stroud et al.

Title Page

Abstract	Introduction
Conclusions	References
Tables	Figures

◄◄   ►►

◄   ►

Back   Close

Full Screen / Esc

Printer-friendly Version

Interactive Discussion

representative case studies for the transboundary transport of air masses to the study region from the southwest. Both case studies are for Harrow; thus, emissions from the Detroit-Windsor air shed are not involved. The case study periods (27 June, 8 July) were also selected for times when the ATOFMS PMF analysis in McGuire et al. (2011) diagnosed a long-range "Transport" factor. The "Transport" factor consisted of three highly-aged single-particle types, namely aged carbonaceous particles (BC and OC cores) with significant coatings of sulphate, ammonium, and oxidized organic fragments and two aged dust particle types. It was hypothesized that the transport mechanism could either be transport aloft over Lake Erie followed by fumigation during the breakdown of the stable marine surface layer on passage over land near Harrow or near-surface transport across Lake Erie followed by on-shore flow behind a lake-breeze front. AURAMS simulations should be able to provide further guidance to support one of these pathways or else to recommend other transport pathways.

On 8 July at Harrow, the POA NMB was −73 % for the period from 10:00-14:50 EST. Back trajectories suggest the surface air had originated in the US Midwest and passed over the Toledo airshed (see SI, CS 2a). This is consistent with the AURAMS PM_1 POA surface distribution (Fig. 11), which shows a surface plume originating from the Toledo urban area in addition to a point-source plume originating just south of Toledo. (Note that this case study for Harrow is simultaneous with the urban-plume case study for Bear Creek discussed in the previous section (cf. Fig. 10).) The vertical cross section at Harrow at 18:00 UTC, which is perpendicular to the surface wind direction, shows an elevated POA layer (∼1000 m) which is likely a signature of longer-range transport. A look at the 870-m layer horizontal distribution showed some directional shear compared to surface and a source of the elevated layer from the Monroe power plant, which is located at the west end of Lake Erie to the northeast of Toledo (Fig. 11). It appears that after advection of the elevated polluted layer over Lake Erie to the warmer land near Harrow, the elevated POA layer was mixed down to the surface, resulting in the increase in modelled POA at the surface. Thus, the model suggests that Harrow was impacted by POA emissions from both Toledo and the Monroe power plant that were

transported across Lake Erie at different vertical levels before mixing down to the surface. No model POA plumes were observed at the surface or aloft upwind of the Toledo or Monroe POA sources. CO was also underpredicted to a greater degree than the CO campaign-mean at Harrow (NMBs of −25 % vs. 2 %), so the cause of the CO and POA underprediction may be common. Note that the measurement-derived HOA may also include some SOA from the oxidation of long-carbon-chain organic compounds in the NOx-rich plumes, thus exaggerating the model's POA underprediction.

Another interesting case period identified by the ATOFMS PMF and labelled long-range "Transport" was on 27 June at Harrow (Table 11). The POA NMB for the period from 10:30–14:00 EST was +17 %, which can be considered good model-measurement agreement. Back trajectories originated over the US Midwest (see SI, CS 2b). The measured HOA and modelled POA means were $0.40 \pm 0.14\,\mu g\,m^{-3}$ and $0.47 \pm 0.10\,\mu g\,m^{-3}$, respectively. The AURAMS POA surface distribution and cross-section (Fig. 12) perpendicular to the surface wind direction on June 27 at 13 EST (18:00 UTC) showed evidence for the transport of an elevated plume (600–1100 m) over Lake Erie followed by fumigation to the Harrow surface site. Figure 12 shows the AURAMS POA horizontal distribution at 815 m and vertical cross section parallel to the surface wind direction at the same time. The elevated plume originated in the model from the Monroe power-generation plant. A vertical cross section (not shown) perpendicular to but further upwind (southwest) of the power-plant source did not show signs of this elevated plume aloft. The mixing heights predicted over land in the cross section are similar to the LIDAR PBL heights measured at Ridgetown. The modelled and measured SO_4 values listed in Table 11 were higher than the campaign-mean values (i.e., 7.4 vs. $3.3\,\mu g\,m^{-3}$ and 4.5 vs. $2.8\,\mu g\,m^{-3}$). The SO_4 NMB value of 64 % suggests the model plume may have more directly impacted the Harrow location than was observed. The high POA in the modelled power plant emissions coupled with the high modelled SO_4 may partially explain the model positive bias for this case compared to the 8 July case. The NMB value for CO was low (−11 %) and for BC was a typical value (−77 %). Point sources in the model do not emit large amounts of either CO or BC. Thus, the

Title Page

Abstract | Introduction

Conclusions | References

Tables | Figures

|◄ | ►|

◄ | ►

Back | Close

Full Screen / Esc

Printer-friendly Version

Interactive Discussion

Title Page

Abstract | Introduction

Conclusions | References

Tables | Figures

◀ | ▶

◀ | ▶

Back | Close

Full Screen / Esc

Printer-friendly Version

Interactive Discussion

interpretation from the model results is consistent with the "transport aloft" hypothesis suggested in McGuire et al. (2011) for the longer-range "Transport" factor.

Collectively, these two cases showed a mean PM_1 POA NMB in the range from +17 % to −73 %, with the positive bias representing a period when the model predicted higher SO_4 and the negative bias representing a period when the model underpredicted CO and SO_4. Overall, the wind direction from the west to southwest was the second-most frequent direction during the campaign period, and wind speeds for these times tended to be higher than those from the northwest (Sills et al., 2011). These two cases suggest that frequent modelled POA underpredictions for transboundary transport flow from the US midwest are also contributing to the campaign-mean negative bias at Harrow (Table 7).

3.8.3 Biomass-burning influence

Table 12 lists two cases when Harrow sampled biomass-burning-influenced air. The model POA averages were low, as AURAMS did not account for emissions from biomass-burning events. The single-particle ATOFMS PMF analysis on 6 July showed influence from a "biomass-burning" factor (McGuire et al., 2011). The AMS PMF spectra were ambiguous for the biomass-burning periods (Slowik et al., 2011) and the factorization routine did not calculate a unique BBOA factor. However, it is likely that some non-quantified amount of the HOA is related to biomass burning as HOA does correlate with acetonitrile and potassium which are tracers for biomass burning (Aiken et al., 2010). HOA also correlates with gaseous aromatics so a mix of influences is likely. Model comparison with the HOA factor results in NMB values of −71 % and −94 % for the 7 July and 6 July periods, respectively. The mesoscale analysis and high-resolution back trajectories can be found in the SI (see case 3ab). These cases also contribute to the overall model POA underprediction at Harrow and support the need to include day-specific biomass burning emissions in AURAMS.

3.8.4 Regional background from the north

Table 13 lists two representative cases for Bear Creek sampling air masses from the north with moderate winds speeds (see SI, case 4ab for mesoscale analysis and back trajectories). Northwest was the predominant wind direction for Bear Creek. There was no indication of influence from local pollution sources or biomass burning in the measurements. Model and measured mass concentrations were in the range 0.1 to 0.2 $\mu g \, m^{-3}$, with only small NMB values of $-19\,\%$ and $1\,\%$. This good level of agreement suggests that rural ORM and ORAA POA sources to the north of the study region are represented well in the model.

3.9 Recommendations for future work

Overall, the methodology of using only four PM chemical speciation profiles (for ORM, ORAA, minor point and major point sources) employed in this study to speciate primary PM emissions resulted in reasonable model performance. The general trend was for model underprediction at higher measured HOA, model overestimation at lower measured HOA, and unbiased model results at mean HOA. However, in the future, modelling specific source plumes for source apportionment studies will require further development and use of source-specific (SCC-based) PM chemical speciation profiles (e.g., POA fractions from coal-combustion vs. natural-gas-combustion plumes, separation of diesel from gasoline combustion).

It would be beneficial to design future studies so that additional chemical mass balance analysis could be performed on source-specific marker species. This would complement the PMF analysis done here. Furthermore, it would be enlightening to perform "tagged" source simulations to compare with the interpretations from a CMB analysis. Together these future studies would help to better characterize the bias for our case study periods.

The magnitude of the area POA sources in the US and Canadian inventories suggests that more effort should be dedicated to reducing uncertainties in these sources

(food cooking, road and soil dust). Work should also be done in parallel to continue to develop both improved and new Canadian spatial and temporal surrogates at finer resolutions (e.g., add more road-type spatial surrogates, improve meat-cooking surrogates for commercial and residential sectors). The combination of (1) higher urban-scale POA and BC emissions from diesel combustion, (2) more structured (i.e., less smooth) spatial allocation of area POA emissions in urban areas (food cooking, road dust), and (3) dynamic POA evaporation based on volatility would help the model trends in terms of magnitude and bias from urban to rural scales. In addition, work should continue with adding biomass-burning emissions capabilities.

4   Summary and conclusions

Primary organic aerosol (POA), which is defined as directly emitted organic aerosol, is typically an important component of atmospheric PM in North America, but it has received less attention to date than secondary organic aerosol. Observations from the 2007 Border Air Quality and Meteorology Study (BAQS-Met 2007) in southern Ontario, Canada, a region of complex summertime mesoscale circulations, have been used to evaluate Environment Canada's regional chemical transport model predictions of POA for the BAQS-Met period. Particle-component-based factor analysis was applied to aerosol mass spectrometer measurements made at one urban site (Windsor, ON) and two rural sites (Harrow and Bear Creek, ON) to derive sub-micron hydrocarbon-like organic aerosol (HOA) factors. Co-located CO, $PM_{2.5}$ BC, and PM_1 SO_4 measurements were also used to evaluate and interpret model results along with surface meteorological mesoscale analyses and high-resolution back trajectories. The richness of the measurement data set permitted a detailed diagnostic model evaluation to be performed, and the fact that POA, BC, and CO are inert or quasi-inert allowed model representations of emissions, transport and diffusion, and removal to be examined without the additional complications of atmospheric chemistry.

An analysis of the POA emissions inventory for summer conditions in Ontario highlights the diversity of OA sources with surprisingly large contributions from ORAA sources such as food cooking, tractor fuel combustion, and road and soil dust, in addition to the well recognized ORM fuel combustion sources. An analysis of the PM_1 POA emissions for the Detroit/Windsor airshed showed contributions of 47 % from ORAA sources, 38 % from point sources, and 15 % from ORM sources. In the study area, many urban and point emissions lie on the shorelines of the Great Lakes and the Detroit River. The influence of the mesoscale lake-breeze fronts and circulations on the dispersion of emissions is very complex in this region in the summer and creates a challenge and necessity to model POA at high resolution in order to capture the spatial structure of local atmospheric flows. A common flow pattern for southwestern Ontario in the summer is brisk winds from the southwest, which results in longer-range transport of air originating from the US Midwest plus superposition of emissions from sources along the shores of Lake Erie. An analysis of the POA emissions inventory was performed for Indiana, a nearby upwind US state for this flow direction, which showed POA emissions dominated by ORAA source (67 %) and point sources (26 %) and a smaller contribution from ORM sources (7 %).

In Windsor, Ontario, a small city (population $\sim$200 000) adjacent to Detroit (city population $\sim$1000 000), Michigan, the BAQS-Met campaign-mean modelled POA and measurement-derived HOA values were very similar at $1.1 \pm 0.9\,\mu g\,m^{-3}$ and $1.2 \pm 1.0\,\mu g\,m^{-3}$, respectively. This is excellent agreement considering the complexity of the sources and meteorology in this region. However, the nightime statistics in Windsor showed a larger POA overprediction. The largest overpredictions were found to occur in stable model surface layers on calm nights and resulted in the accumulation of urban POA emissions in the lowest model grid layer. For Windsor, the model also overpredicted POA levels at lower BC to HOA ratios and underpredicted POA levels at higher BC to HOA ratios. This trend suggests that on-road diesel emissions, which are rich in BC relative to POA, may be under-represented in the emissions inventories that were used for modelling. Some evidence for this was shown by examining model

predictions for air masses originating from southern Detroit, which is a heavily indus-
trialized area with extensive use of diesel trucks. Southern Windsor also includes the
major highway for diesel trucks crossing one of the busiest Canada/US border cross-
ings. Conversely, some of the area sources that are richer in POA relative to BC were
5 associated with POA overpredictions.

Other scatter plots for Windsor showed a trend of increasing model POA overpre-
diction at lower HOA concentrations. This could result from inaccuracies in the spa-
tial surrogate fields used by the SMOKE emissions processing system to allocation
area-source emissions in space, with under-weighting over urban centers, or from the
10 inability of a model with relatively coarse grid spacing to resolve the spatial distribution
of emissions at urban scales. The trend of overprediction at lower HOA mass concen-
trations is also consistent with the need to include the POA evaporation process as
proposed by Robinson et al. (2010).

At Windsor and Harrow, a few time periods were observed when the high-resolution
15 (2.5-km) model captured the position of high SO_4 power plant plumes accurately.
These periods were frequently also times with significant POA overpredictions. This
suggests the POA emission factor in our PM chemical speciation profile for SO_4-rich
point sources may be too high. Additional time periods were observed when the model
over-predicted both PM_1 SO_4 and POA and these likely reflect additional uncertainties
20 associated with predicting plume placement and boundary layer vertical mixing.

At the rural Bear Creek supersite, POA underprediction was also observed for cases
of outflow from the Detroit-Windsor urban area, whereas there was good agreement
in general at Bear Creek for periods when clean background air flowed into the study
region from the north. Measurement-derived HOA was also considerably lower at Bear
25 Creek than at Windsor or Harrow.

Campaign-mean POA statistics were considerably worse at the rural Harrow super-
site than at either Windsor or Bear Creek. At Harrow, the case studies that were found
to contribute to the campaign-mean POA underprediction were: (1) outflow periods
from Detroit-Windsor, (2) transboundary flow periods from the US Midwest, and (3)

Title Page

Abstract | Introduction

Conclusions | References

Tables | Figures

◀ | ▶

◀ | ▶

Back | Close

Full Screen / Esc

Printer-friendly Version

Interactive Discussion

biomass-burning periods. Meteorological influences associated with the frequent lake-breeze conditions likely also contributed to uncertainties at Harrow, which is situated close to the north shore of Lake Erie, but we tried to isolate case-study time periods when the model meteorology was representative of common flow patterns identified in the mesoscale meteorological analysis of Sills et al. (2011).

The good POA agreement at Windsor and POA underprediction at Harrow vs. the CO overprediction at Windsor and good CO agreement at Harrow appears to be in conflict and is not easy to reconcile. One possible explanation could be an under-estimate in the ORAA POA emissions for urban areas (possibly related to the spatial surrogate fields used for spatial disaggregation of food cooking and dust emissions) and an under-representation of urban-scale vertical mixing in the lowest model layers, especially at night. In addition, the consistent underprediction of $PM_{2.5}$ BC at all sites needs to be considered. Diesel emissions underestimates may be the cause of the BC underpredictions as has been hypothesized in other studies as well (Ying et al., 2007; Liggio et al., 2011).

List of acronyms

a.g.l.	above ground level
AMS	aerosol mass spectrometer
AQ	air quality
ATOFMS	Aerosol time of flight mass spectrometer
AURAMS	A Unified Regional Air-quality Modelling System
BAQS-Met	Border Air Quality and Meteorology Study
BBOA	biomass burning OA
BC	black carbon (synonymous with elemental carbon)
CLBC	chemical lateral boundary condition
CM	crustal material
CMB	carbon mass balance
CO	carbon monoxide
CRUISER	Canadian Regional and Urban Investigation System for Environmental Research
CS	case study
CTM	chemical transport model
EPA	Environmental Protection Agency
EST	Eastern Standard Time
GEM	Global Multiscale Model (Canada's meteorology model)
HOA	hydrocarbon-like OA
IVOC	intermediate volatile organic compound
LIDAR	Light Detection and Ranging
MAAP	multi-angle absorption photometer
NEI	national emissions inventory
NMB	normalized mean bias
OA	organic aerosol
OC	organic carbon
ON	Ontario
OOA	oxygenated OA
ORAA	off-road and area
ORM	on-road mobile
PAHs	polycyclic aromatic hydrocarbons
POA	primary organic aerosol
PBL	planetary boundary layer
PM	particulate matter
PM_1	PM with aerodynamic diameter less than or equal to 1 µm
$PM_{2.5}$	PM with aerodynamic diameter less than or equal to 2.5 µm
PMF	positive matrix factorization
POA	primary organic aerosol
POC	primary organic carbon
RMSE	root mean square error
SCC	source classification category
SMOKE	Sparse Matrix Operator Kernel Emissions processing system
SOA	secondary organic aerosol
SO_4	sulphate aerosol
UNKN	unknown PMF factor

References

Aiken, A. C., de Foy, B., Wiedinmyer, C., DeCarlo, P. F., Ulbrich, I. M., Wehrli, M. N., Szidat, S., Prevot, A. S. H., Noda, J., Wacker, L., Volkamer, R., Fortner, E., Wang, J., Laskin, A., Shutthanandan, V., Zheng, J., Zhang, R., Paredes-Miranda, G., Arnott, W. P., Molina, L. T., Sosa, G., Querol, X., and Jimenez, J. L.: Mexico city aerosol analysis during MILAGRO using high resolution aerosol mass spectrometry at the urban supersite (T0) – Part 2: Analysis of the biomass burning contribution and the non-fossil carbon fraction, Atmos. Chem. Phys., 10, 5315–5341, doi:10.5194/acp-10-5315-2010, 2010.

Andreae, M. O. and Gelencsér, A.: Black carbon or brown carbon? The nature of light-absorbing carbonaceous aerosols, Atmos. Chem. Phys., 6, 3131–3148, doi:10.5194/acp-6-3131-2006, 2006.

Bhave, P. V., Pouliot, G. A., and Zheng, M.: Diagnostic model evaluation for carbonaceous $PM_{2.5}$ using organic markers measured in the southeastern US, Environ. Sci. Technol., 41, 1577–1583, 2007.

Boström, C.-E., Gerde, P., Hanberg, A., Jernström, B., Johansson, C., Kyrklund, T., Rannug, A., Törnqvist, M., Victorin, K., andWesterholm, R.: Cancer risk assessment, indicators, and

Title Page

Abstract | Introduction

Conclusions | References

Tables | Figures

◄ | ►|

◄ | ►

Back | Close

Full Screen / Esc

Printer-friendly Version

Interactive Discussion

guidelines for polycyclic aromatic hydrocarbons in the ambient air, Environ. Health. Persp., 110 (Suppl. 3), 451–488, 2002.

Brook, J., Makar, P., Sills, D., Hayden, K., and McLaren, R.: The Border Air Quality and Meteorology Study: Exploring the nature of air quality over southern Ontario, in preparation, 2011.

CEP (Carolina Environmental Program): Sparse Matrix Operator Kernel Emissions (SMOKE) processing system, http://www.smoke-model.org/index.cfm, University of North Carolina, Chapel Hill, 2011.

Chan, T. W., Huang, L., Leaitch, W. R., Sharma, S., Brook, J. R., Slowik, J. G., Abbatt, J. P. D., Brickell, P. C., Liggio, J., Li, S.-M., and Moosmüller, H.: Observations of OM/OC and specific attenuation coefficients (SAC) in ambient fine PM at a rural site in central Ontario, Canada, Atmos. Chem. Phys., 10, 2393–2411, doi:10.5194/acp-10-2393-2010, 2010.

Chen, J., Griffin, R. J., Grini, A., and Tulet, P.: Modeling secondary organic aerosol formation through cloud processing of organic compounds, Atmos. Chem. Phys., 7, 5343–5355, doi:10.5194/acp-7-5343-2007, 2007.

Côté, J., Gravel, S., Méthot, A., Patoine, A., Roch, M., and Staniforth, A.: The operational CMC-MRB global environmental multiscale (GEM) model. Part I: Design considerations and formulation, Mon. Weather Rev., 126, 1373–1395, 1998.

De Gouw, J. A., Middlebrook, A. M., Warneke, C., Ahmadov, R., Atlas, E. L., Bahreini, R., Blake, D. R., Brock, C. A., Brioude, J., Fahey, D. W., Fehsenfeld, F. C., Holloway, J. S., Le Henaff, M., Lueb, R. A., McKeen, S. A., Meagher, J. F., Murphy, D. M., Paris, C., Parrish, D. D., Perring, A. E., Pollack, I. B., Ravishankara, A. R., Robinson, A. L., Ryerson, T. B., Schwarz, J. P., Spackman, J. R., Srinivasan, A., and Watts L. A.: Organic aerosol formation downwind from the Deepwater Horizon oil spill, Science, 331, 1295–1299, 2011.

Dreyfus, M. A., Adou, K., Zucker, S. M., and Johnston, M. V.: Organic aerosol source apportionment from highly time-resolved molecular composition measurements, Atmos. Environ., 43, 2901–2910, 2009.

Eldering, A. and Cass, G. R.: Source-oriented model for air pollutant effects on visibility, J. Geophys. Res.-Atmos., 101, 19343–19369, 1996.

Environment Canada and Health Canada: Canadian Smog Science Assessment, available from first author upon request, 2011.

Environment Canada: AQSC-10-018 Provision of Atmospheric and Emission Modelling Services for Input into Human Health Assessments: Final report on Environment Canada's

achievements under ILA 2007-02 (4500194215) related to biodiesel atmospheric modelling, unpublished report, Air Quality Modelling Applications Sections, Meteorological Service of Canada, 97 p., available upon request, 2011.

Gong, S. L., Barrie, L. A., Blanchet, J.-P., von Salzen, K., Lohmann, U., Lesins, G., Spacek, L., Zhang, L. M., Girard, E., Lin, H., Leaitch, R., Leighton, H., Chylek, P., and Huang, P.: Canadian aerosol module: A size-segregated simulation of atmospheric aerosol processes for climate and air quality models 1. module development, J. Geophys. Res.-Atmos., 108, AAC 3-1 AAC 3-16, 2003.

Gong, W., Dastoor, A. P., Bouchet, V. S., Gong, S., Makar, P. A., Moran, M. D., and Pabla, B., Ménard, S., Crevier, L., Cousineau, S., and Venkatesh, S.: Cloud processing of gases and aerosols in a regional air quality model (AURAMS), Atmos. Res., 82, 248–275, 2006.

Grell, G., Freitas, S. R., Stuefer, M., and Fast, J.: Inclusion of biomass burning in WRF-Chem: impact of wildfires on weather forecasts, Atmos. Chem. Phys., 11, 5289–5303, doi:10.5194/acp-11-5289-2011, 2011.

Hu, D., Bian, Q., Lau, A. K. H., and Yu, J. Z.: Source apportioning of primary and secondary organic carbon in summer $PM_{2.5}$ in Hong Kong using positive matrix factorization of secondary and primary organic tracer data, J. Geophys. Res.-Atmos., 115, D16204, doi:10.1029/2009JD012498, 2010.

IPCC AR4 WG1, Solomon, S., Qin, D., Manning, M., Chen, Z., Marquis, M., Averyt, K. B., Tignor, M., and Miller, H. L., eds.: Climate Change 2007: The Physical Science Basis, Contribution of Working Group I to the Fourth Assessment Report of the Intergovernmental Panel on Climate Change, Cambridge University Press, ISBN, 978-0-521-88009-1, 2007.

Kelly, J., Makar, P. A., and Plummer, D. A.: Projections of mid-century summer air-quality for North America: effects of changes in climate and precursor emissions, Atmos. Chem. Phys. Discuss., 12, 3875–3940, doi:10.5194/acpd-12-3875-2012, 2012.

Lane, T. E., Pinder, R. W., Shrivastava, M., Robinson, A. L., and Pandis, S. N.: Source contributions to primary organic aerosol: Comparison of the results of a source-resolved model and the chemical mass balance approach, Atmos. Environ., 41, 3758–3776, 2007.

Lanz, V. A., Alfarra, M. R., Baltensperger, U., Buchmann, B., Hueglin, C., and Prévôt, A. S. H.: Source apportionment of submicron organic aerosols at an urban site by factor analytical modelling of aerosol mass spectra, Atmos. Chem. Phys., 7, 1503–1522, doi:10.5194/acp-7-1503-2007, 2007.

Levy, I., Makar, P. A., Sills, D., Zhang, J., Hayden, K. L., Mihele, C., Narayan, J., Moran, M.

Evaluation of chemical transport model predictions

C. A. Stroud et al.

Title Page

Abstract | Introduction

Conclusions | References

Tables | Figures

◄◄ | ►►

◄ | ►

Back | Close

Full Screen / Esc

Printer-friendly Version

Interactive Discussion

D., Sjostedt, S., and Brook, J.: Unraveling the complex local-scale flows influencing ozone patterns in the southern Great Lakes of North America, Atmos. Chem. Phys., 10, 10895–10915, doi:10.5194/acp-10-10895-2010, 2010.

Li, S.-M., Liggio, J., Graham, L., Lu, G., Brook, J., Stroud, C., Zhang, J., Makar, P., and Moran, M. D.: Condensational uptake of semivolatile organic compounds in gasoline engine exhaust onto pre-existing inorganic particles, Atmos. Chem. Phys., 11, 10157–10171, doi:10.5194/acp-11-10157-2011, 2011.

Liggio, J., Li, S.-M., and McLaren, R.: Reactive uptake of glyoxal by particulate matter, J. Geophys. Res. Atmos., 110, 1–13, 2005.

Liggio, J., Gordon, M., Brook, J. R., Smallwood, G., Li, S. M., Stroud, C. A., Staebler, R., Lu, G., Lee, P., and Taylor, B.: Emissions of black carbon from gasoline vehicles is underestimated: Insights from near and on-road measurements, Environ. Sci. Technol., accepted, 2012.

Makar, P. A., Gravel, S., Chirkov, V., Strawbridge, K. B., Froude, F., Arnold, J., and Brook, J. : Heat flux, urban properties, and regional weather, Atmos. Environ., 40, 2750–2766, 2006.

Makar, P. A., Zhang, J., Gong, W., Stroud, C., Sills, D., Hayden, K. L., Brook, J., Levy, I., Mihele, C., Moran, M. D., Tarasick, D. W., He, H., and Plummer, D.: Mass tracking for chemical analysis: the causes of ozone formation in southern Ontario during BAQS-Met 2007, Atmos. Chem. Phys., 10, 11151–11173, doi:10.5194/acp-10-11151-2010, 2010a.

Makar, P. A., Gong, W., Mooney, C., Zhang, J., Davignon, D., Samaali, M., Moran, M. D., He, H., Tarasick, D. W., Sills, D., and Chen, J.: Dynamic adjustment of climatological ozone boundary conditions for air-quality forecasts, Atmos. Chem. Phys., 10, 8997–9015, doi:10.5194/acp-10-8997-2010, 2010b.

Mauderly, J. L. and Chow, J. C.: Health effects of organic aerosols, Inhal. Toxicol. , 20, 257–288, 2008.

McGuire, M. L., Jeong, C.-H., Slowik, J. G., Chang, R. Y.-W., Corbin, J. C., Lu, G., Mihele, C., Rehbein, P. J. G., Sills, D. M. L., Abbatt, J. P. D., Brook, J. R., and Evans, G. J.: Elucidating determinants of aerosol composition through particle-type-based receptor modeling, Atmos. Chem. Phys., 11, 8133–8155, doi:10.5194/acp-11-8133-2011, 2011.

Mohr, C., Huffman, J. A., Cubison, M. J., Aiken, A. C., Docherty, K. S., Kimmel, J. R., Ulbrich, I. M., Hannigan, M., and Jimenez, J. L.: Characterization of primary organic aerosol emissions from meat cooking, trash burning, and motor vehicles with high-resolution aerosol mass spectrometry and comparison with ambient and chamber observations, Environ. Sci. Technol., 43, 2443–2449, 2009.

Title Page

Abstract | Introduction

Conclusions | References

Tables | Figures

◀◀ | ▶▶

◀ | ▶

Back | Close

Full Screen / Esc

Printer-friendly Version

Interactive Discussion

Pachon, J. E., Balachandran, S., Hu, Y., Weber, R. J., Mulholland, J. A., and Russell, A. G.: Comparison of SOC estimates and uncertainties from aerosol chemical composition and gas phase data in Atlanta, Atmos. Environ., 44, 3907–3914, 2010.

Pankow, J. F.: An absorption model of gas/particle partitioning of organic compounds in the atmosphere, Atmos. Environ., 28, 185–188, 1994.

Pope III, C. A. and Dockery, D. W.: Health effects of fine particulate air pollution: Lines that connect, J. Air Waste Ma., 56, 709–742, 2006.

Robinson, A. L., Grieshop, A. P., Donahue, N. M., and Hunt, S. W.: Updating the conceptual model for fine particle mass emissions from combustion systems, J. Air Waste Ma., 60, 1204–1222, 2010.

Sage, A. M., Weitkamp, E. A., Robinson, A. L., and Donahue, N. M.: Evolving mass spectra of the oxidized component of organic aerosol: results from aerosol mass spectrometer analyses of aged diesel emissions, Atmos. Chem. Phys., 8, 1139–1152, doi:10.5194/acp-8-1139-2008, 2008.

Samaali, M., Bouchet, V. S., Moran, M. D., and Sassi, M.: Application of a tagged-species method to source apportionment of primary $PM_{2.5}$ components in a regional air quality model, Atmos. Environ., 45, 3835–3847, doi:10.1016/j.atmosenv.2011.04.007, 2011.

Schauer, J. J., Kleeman, M. J., Cass, G. R., and Simoneit, B. R. T.: Measurement of emissions from air pollution sources. 2. C1 through C30 organic compounds from medium duty diesel trucks, Environ. Sci. Technol., 33, 1578–1587, 1999.

Sills, D. M. L., Brook, J. R., Levy, I., Makar, P. A., Zhang, J., and Taylor, P. A.: Lake breezes in the southern Great Lakes region and their influence during BAQS-Met 2007, Atmos. Chem. Phys., 11, 7955–7973, doi:10.5194/acp-11-7955-2011, 2011.

Slowik, J. G., Stroud, C., Bottenheim, J. W., Brickell, P. C., Chang, R. Y.-W., Liggio, J., Makar, P. A., Martin, R. V., Moran, M. D., Shantz, N. C., Sjostedt, S. J., van Donkelaar, A., Vlasenko, A., Wiebe, H. A., Xia, A. G., Zhang, J., Leaitch, W. R., and Abbatt, J. P. D. . Characterization of a large biogenic secondary organic aerosol event from eastern Canadian forests. Atmos. Chem. Phys., 10, 2825–2845, doi:10.5194/acp-10-2825-2010, 2010.

Slowik, J. G., Brook, J., Chang, R. Y.-W., Evans, G. J., Hayden, K., Jeong, C.-H., Li, S.-M., Liggio, J., Liu, P. S. K., McGuire, M., Mihele, C., Sjostedt, S., Vlasenko, A., and Abbatt, J. P. D.: Photochemical processing of organic aerosol at nearby continental sites: contrast between urban plumes and regional aerosol, Atmos. Chem. Phys., 11, 2991–3006, doi:10.5194/acp-11-2991-2011, 2011.

Title Page

Abstract | Introduction

Conclusions | References

Tables | Figures

◄◄ | ►►

◄ | ►

Back | Close

Full Screen / Esc

Printer-friendly Version

Interactive Discussion

Strawbridge, K. B.: Scanning lidar: A means of characterizing the Noranda-Horne smelter plume, Geochemistry: Exploration, Environment, Analysis, 6, 121–129, 2006.

Stroud, C. A., Morneau, G., Makar, P. A., Moran, M. D., Gong, W., Pabla, B., Zhang, J., Bouchet, V. S., Fox, D., Venkatesh, S., Wang, D., and Dann, T.: OH-reactivity of volatile organic compounds at urban and rural sites across Canada: Evaluation of air quality model predictions using speciated VOC measurements, Atmos. Environ., 42(33), 7746–7756, 2008.

Stroud, C. A., Makar, P. A., Moran, M. D., Gong, W., Gong, S., Zhang, J., Hayden, K., Mihele, C., Brook, J. R., Abbatt, J. P. D., and Slowik, J. G.: Impact of model grid spacing on regional- and urban- scale air quality predictions of organic aerosol, Atmos. Chem. Phys., 11, 3107–3118, doi:10.5194/acp-11-3107-2011, 2011.

Takegawa, N., Miyakawa, T., Kondo, Y., Jimenez, J. L., Zhang, Q., Worsnop, D. R., and Fukuda, M.: Seasonal and diurnal variations of submicron organic aerosol in Tokyo observed using the aerodyne aerosol mass spectrometer, J. Geophys. Res.-Atmos., 111, doi:10.1029/2005JD006515, 2006.

Takegawa, N., Miyakawa, T., Kondo, Y., Blake, D. R., Kanaya, Y., Koike, M., Fukuda, M., Komazaki, Y., Miyazaki, Y., Shimono, A., and Takeuchi, T.: Evolution of submicron organic aerosol in polluted air exported from tokyo, Geophys. Res. Lett., 33, doi:10.1029/2006GL025815, 2006.

US EPA: SPECIATE program, http://www.epa.gov/ttn/chief/emch/speciation, last access: November 2011, 2011.

Williams, B. J., Goldstein, A. H., Kreisberg, N. M., Hering, S. V., Worsnop, D. R., Ulbrich, I. M., Docherty, K. S., and Jimenez, J. L.: Major components of atmospheric organic aerosol in southern California as determined by hourly measurements of source marker compounds, Atmos. Chem. Phys., 10, 11577–11603, doi:10.5194/acp-10-11577-2010, 2010.

Ying, Q., Fraser, M. P., Griffin, R. J., Chen, J., and Kleeman, M. J.: Verification of a source-oriented externally mixed air quality model during a severe photochemical smog episode, Atmos. Environ., 41, 1521–1538, 2007.

Zhang, J., Gong, W., Leaitch, W. R., and Strapp, J. W.: Evaluation of modeled cloud properties against aircraft observations for air quality applications, J. Geophys. Res. Atmos., 112, D10S16, doi:10.1029/2006JD007596, 2007.

Zhang, H. and Ying, Q.: Source apportionment of airborne particulate matter in southeast Texas using a source-oriented 3D air quality model, Atmos. Environ., 44, 3547–3557, 2010.

Zhang, Q., Rami Alfarra, M., Worsnop, D. R., Allan, J. D., Coe, H., Canagaratna, M. R., and

Title Page

Abstract | Introduction

Conclusions | References

Tables | Figures

◀ | ▶

◀ | ▶

Back | Close

Full Screen / Esc

Printer-friendly Version

Interactive Discussion

Jimenez, J. L.: Deconvolution and quantification of hydrocarbon-like and oxygenated organic aerosols based on aerosol mass spectrometry, Environ. Sci. Technol., 39(13), 4938–4952, 2005a.

Zhang, Q., Worsnop, D. R., Canagaratna, M. R., and Jimenez, J. L.: Hydrocarbon-like and oxygenated organic aerosols in Pittsburgh: insights into sources and processes of organic aerosols, Atmos. Chem. Phys., 5, 3289–3311, doi:10.5194/acp-5-3289-2005, 2005b.

Zhang, Q., Jimenez, J. L., Canagaratna, M. R., Allan, J. D., Coe, H., Ulbrich, I., Alfarra, M. R., Takami, A., Middlebrook, A. M., Sun, Y. L., Dzepina, K., Dunlea, E., Docherty, K., De-Carlo, P. F., Salcedo, D., Onasch, T., Jayne, J. T., Miyoshi, T., Shimono, A., Hatakeyama, S., Takegawa, N., Kondo, Y., Schneider, J., Drewnick, F., Borrmann, S., Weimer, S., Demerjian, K., Williams, P., Bower, K., Bahreini, R., Cottrell, L., Griffin, R. J., Rautiainen, J., Sun, J. Y., Zhang, Y. M., and Worsnop, D. R.: Ubiquity and dominance of oxygenated species in organic aerosols in anthropogenically-influenced Northern Hemisphere midlatitudes, Geophys. Res. Lett., 34, L13801, doi:10.1029/2007GL029979, 2007.

Zhang, Y.: Online-coupled meteorology and chemistry models: history, current status, and outlook, Atmos. Chem. Phys., 8, 2895–2932, doi:10.5194/acp-8-2895-2008, 2008.

Zhang, Y., Sheesley, R. J., Schauer, J. J., Lewandowski, M., Jaoui, M., Offenberg, J. H., Klein-dienst, T. E., and Edney, E. O.: Source apportionment of primary and secondary organic aerosols using positive matrix factorization (PMF) of molecular markers, Atmos. Environ., 43, 5567–5574, 2009.

Zhang, J., Moran, M., Makar, P., Sassi, M., and Zheng, Q.: Investigation of cross-border differences in the spatial distribution of onroad mobile emissions between the US and Canada, poster 13, 19th International Emission Inventory Conference, 27–30 September, San Antonio, Texas (availabe at: http://www.epa.gov/ttn/chief/conference/ei19/poster/jzhang.pdf), 2010.

Table 1. POA emissions inventory for the province of Ontario calculated from the 2006 Canadian $PM_{2.5}$ NEI with the application of SCC-specific PM chemical speciation profiles and sorted by importance into four aggregate source streams (where 1 ton = 0.9072 tonnes).

Source Stream	Ontario 2006 PM Inventory Source Category	$PM_{2.5}$ POC Emissions (tons C yr^{-1})		PM_1 Summer Source-Stream Contribution (% Contribution[2])
		Annual	Summer[1]	
On-road Mobile	Heavy Duty Diesel Vehicles	299	75 A	196 × 0.96 (5 %)
	Light Duty Gasoline Cars	212	53 A	
	Light Duty Gasoline Trucks	180	45 A	
	Heavy Duty Gasoline Vehicles	40	10 A	
	Other On-road Vehicles	50	13 A	
Off-road Mobile	Diesel Agricultural Tractors	958	479 B	1168 × 0.96 (29 %)
	Diesel Agricultural Combines	96	48 B	
	Gasoline Pleasure Craft – Outboard	845	211 A	
	Gasoline Recreational – Snowmobiles	641	0 C	
	Diesel Trains	221	55 A	
	Diesel Trucks for Construction, Mining	79	20 A	
	Other Off-road Mobile Sources	1420	355 A	
Area	Residential Wood Combustion	12,748	0 C	3.477 × 0.73 (64 %)
	Residential Natural Gas	948	0 C	
	Residential Liquid Petroleum Gas and Oil	36	0 C	
	Commercial Fuel Combustion	238	60 A	
	Electric Utility Fuel Combustion	15	4 A	
	Agricultural Production – Mostly Crop Drying and Loading	11	6 B	
	Charcoal Grilling	2.690	1.345 B	
	Description Unavailable	1.822	456 A	
	Dust - Construction	292	146 B	
	- Agriculture	71	36 B	
	- Road Fugitives	2052	1026 B	
	Waste Disposal Burning	270	68 A	
	Industrial Metal Production	733	183 A	
	Industrial Mineral Processes	126	32 A	
	Industrial Petroleum Refining	445	111 A	
	Other Area Sources	14	4 A	
Point	Sum of all major and minor stacks	313	78 A	78 × 0.99 (2 %)
Total		25.452	4.919	

Title Page

Abstract | Introduction

Conclusions | References

Tables | Figures

◀ | ▶

◀ | ▶

Back | Close

Full Screen / Esc

Printer-friendly Version

Interactive Discussion

Printer-friendly Version

Interactive Discussion

[1]Summer total column:

A emissions divided into all 4 seasons equally (÷4)

B emissions only for $1/2$ spring, summer and $1/2$ fall (÷2)

C emissions only in winter

5 [2]Percentage Source Stream Contribution (in brackets) calculated using by summing individual summertime contributions in prior column and applying a PM_1 fraction of $PM_{2.5}$ factor (0.96 for mobile, 0.73 for area, and 0.99 for point source streams).

Table 2. POA inventory for the state of Indiana calculated with the 2005 US $PM_{2.5}$ emissions inventory with the application of SCC-specific PM chemical speciation profiles and sorted by importance into four aggregate source streams.

Source Stream	Indiana 2005 PM Inventory Source Categories	$PM_{2.5}$ POC Emissions (Tons POC yr^{-1})		PM_1 Summer Source Stream Contribution (% Contribution[2])
		Annual	Summer	
On-road Mobile	Heavy Duty Diesel Vehicles	N/A	92 D	204 × 0.96 (7 %)
	Light Duty Gasoline Cars	N/A	51 D	
	Light Duty Gasoline Trucks	N/A	35 D	
	Heavy Duty Gasoline Vehicles	N/A	18 D	
	Other On-road Vehicles	N/A	8 D	
Off-road Mobile	Diesel Agricultural Tractors	N/A	75 D	572 × 0.96 (19 %)
	Diesel Agricultural Combines	N/A	8 D	
	Gasoline Pleasure Craft – Outboard	N/A	81 D	
	Gasoline Recreational Vehicles	N/A	76 D	
	Gasoline Lawn and Garden	N/A	91 D	
	Diesel Construction and Mining	N/A	62 D	
	Forklifts	N/A	18 D	
	Diesel Trains	158	40 A	
	Commercial Marine Vessels	60	15 A	
	Other Off-road Sources	N/A	106 D	
Area	Residential Wood Combustion	2.249	0 C	1.863 × 0.73 (48 %)
	Residential Natural gas	26	0 C	
	Residential Petroleum Gas, Coal, Oil	70	0 C	
	Commercial Fuel Combustion	22	6 A	
	Industrial Fuel Combustion	621	155 A	
	Charcoal Grilling	1.185	593 B	
	Dust - Construction	99	50 B	
	- Agriculture	632	316 B	
	- Road Fugitives	921	460 B	
	Waste Disposal Burning	1.127	282 A	
	Other Area Sources	5	1 A	
Point	Sum of all major and minor stacks (coal-based electric generation units (EGUs), natural gas EGUs, industry natural gas combustion, oil-based commercial boilers, metal production, fibreglass production, coatings, others)	1.070 EGUs + 1.990 non-EGUs	765 A (~1/3 by EGUs)	765 × 0.99 (26 %)
Total		N/A	3.404	

Title Page

Abstract | Introduction

Conclusions | References

Tables | Figures

⏮ | ⏭

◀ | ▶

Back | Close

Full Screen / Esc

Printer-friendly Version

Interactive Discussion

[1] Summer total column:

A emissions divided into all 4 seasons equally ($\div 4$)

B emissions only for $\frac{1}{2}$ spring, summer and $\frac{1}{2}$ fall ($\div 2$)

C emissions only in winter

D emissions calculated from daily US EPA MOBILE6 model output (Summer=91 days)

[2]Percentage Source Stream Contribution (in brackets) calculated using by summing individual summertime contributions in prior column and applying a PM_1 fraction of $PM_{2.5}$ factor (0.96 for mobile, 0.73 for area, and 0.99 for point source streams).

N/A Not Applicable

Table 3. Percentage emission source contributions for different model domains (PM emissions are for PM_1 size range) for July on Monday at 17:00 UTC (12:00 EST).

Species	Source Classification	Detroit 42 km Grid Cell	15 km Domain	2.5 km Domain
PM_1 POA	On-road	15 %	5.8 %	8.4 %
	Off-road + Area	**47 %**	**74 %**	**74 %**
	Minor + Major Point	10 %+28 %=**38 %**	5.5 %+14.9 % = **20 %**	5.2 %+12 % = **17 %**
CO	On-road	**47 %**	**46 %**	**44 %**
	Off-road + Area	**49 %**	**51 %**	**53 %**
	Minor+Major Point	1.8 % + 2.0 %=3.8 %	1.2 % + 1.9 % = 3.1 %	0.7 % + 2.2 % = 2.9 %
PM_1 BC	On-road	**54 %**	**27 %**	**35 %**
	Off-road+Area	31 %	**63 %**	**57 %**
	Minor + Major Point	3.9 + 10.7 %=14.6 %	2.7 + 7.3 % = 10 %	2.2 % + 5.3 % = 7.5 %

Percentages greater than 20 % are highlighted for emphasis.

Table 4. AURAMS PM$_1$ POA model performance statistics for the 2.5-km grid for the urban Windsor site (concentrations in $\mu g\,m^{-3}$).

PM$_1$ POA	Windsor Daytime 09:00–14:00 EST	Windsor Evening and Nighttime 18:00–06:00 EST	Windsor Rush-Hour Periods 06:00–09:00 EST 14:00–18:00 EST
Number of points (15 min averages)	194 13 days 13 days	532 13 days	264
Model POA Average ± Std Dev	1.1 ± 0.9	2.1 ± 2.8	1.6 ± 1.6
PMF HOA Average ± Std Dev	1.2 ± 1.0	1.0 ± 1.0	1.4 ± 2.1
y-Intercept (model value)	0.65	0.85	1.4
Slope	0.39	1.2	0.16
Mean Bias (model-measured)	0.18	1.0	0.16
Normalized Mean Bias	+15 %	+100 %	+1 %
Normalized Mean Error	17 %	140 %	91 %
RMSE	0.31	2.7	2.3
Correlation, R	0.43	0.41	0.20

Evaluation of chemical transport model predictions

C. A. Stroud et al.

Title Page

Abstract | Introduction

Conclusions | References

Tables | Figures

|◄ | ►|

◄ | ►

Back | Close

Full Screen / Esc

Printer-friendly Version

Interactive Discussion

Table 5. AURAMS CO model performance statistics for the 2.5-km grid for the urban Windsor site (mixing ratios in ppbv).

CO	Windsor Daytime 09:00-14:00 EST	Windsor Evening and Nighttime 18:00–06:00 EST	Windsor Rush-Hour Periods 06:00–09:00 EST 14:00–18:00 EST
Number of points (15 min averages)	189 13 days	535 13 days	262 13 days
Model CO Average ± Std Dev	592 ± 405	566 ± 393	665 ± 539
Meas. CO Average ± Std Dev	253 ± 145	285 ± 219	301 ± 318
y-Intercept (model value)	420 ± 58	346 ± 25	474 ± 43
Slope	0.68 ± 0.20	0.77 ± 0.07	0.64 ± 0.10
Mean Bias (model-measured)	+339	+281	+364
Normalized Mean Bias	+134 %	+99 %	+121 %
Normalized Mean Error	142 %	107 %	137 %
RMSE	520	455	628
Correlation, R	0.24	0.43	0.38

Table 6. AURAMS PM$_{2.5}$BC model performance statistics for the 2.5-km grid for the urban Windsor site (concentrations in $\mu g\,m^{-3}$).

PM$_{2.5}$BC	Windsor Daytime 09:00–14:00 EST	Windsor Evening and Nighttime 18:00–06:00 EST	Windsor Rush-Hour Periods 06:00–09:00 EST 14:00–18:00 EST
Number of points (15 min averages)	190 13 days	535 13 days	263 13 days
Model BC Average ± Std Dev	0.70 ± 0.60	0.83 ± 0.82	0.88 ± 0.88
Meas BC Average ± Std Dev	1.3 ± 1.3	1.4 ± 1.5	1.3 ± 1.4
y-Intercept (model value)	0.45 ± 0.06	0.50 ± 0.04	0.36 ± 0.06
Slope	0.19 ± 0.03	0.24 ± 0.02	0.41 ± 0.03
Mean Bias (model-measured)	−0.65	−0.57	−0.38
Normalized Mean Bias	−48 %	−41 %	−30 %
Normalized Mean Error	59 %	61 %	55 %
RMSE	1.38	1.47	1.12
Correlation, R	0.42	0.43	0.64

Table 7. AURAMS PM$_1$ POA model performance statistics for the 2.5-km grid for the rural Harrow and Bear Creek sites (concentrations in µg m^{-3}).

PM1 POA	Harrow Daytime 09:00–18:00 EST	Harrow Night-Time 18:00–09:00 EST	Bear Creek Daytime 09:00–18:00 EST	Bear Creek Nighttime 18:00–09:00 EST
Number of points	1828 (15 min avges) 23 days	3480 23 days	297 (3 min avges) 12 days	538 12 days
Model POA Average ± Std Dev	0.3 ± 0.2	0.4 ± 0.3	0.24 ± 0.21	0.36 ± 0.23
PMF HOA Average ± Std Dev	0.8 ± 0.7	0.9 ± 0.9	0.31 ± 0.39	0.32 ± 0.31
y-Intercept (model value)	0.246	0.336	0.14	0.29
Slope	0.058	0.116	0.32	0.21
Mean Bias	−0.48	−0.45	−0.07	0.039
Normalized Mean Bias	−62 %	−51 %	−23 %	+12 %
Normalized Mean Error	69 %	69 %	63 %	73 %
RMSE	0.87	0.93	0.32	0.34
Correlation, R	0.23	0.32	0.58	0.28

Table 8. AURAMS CO model performance statistics for the 2.5-km grid for the rural Harrow and Bear Creek sites (concentrations in ppbv).

CO	Harrow Daytime 09:00–18:00 EST	Harrow Nighttime 18:00–09:00 EST	Bear Creek Daytime 09:00–18:00 EST	Bear Creek Nighttime 18:00–09:00 EST
Number of points	1514 (15 min avges) 23 days	3139 23 days	227 (3 min avges) 12 days	477 12 days
Model CO Average ± Std Dev	180 ± 49	192 ± 62	172 ± 44	172 ± 44
Meas. CO Average ± Std Dev	197 ± 87	204 ± 82	199 ± 97	210 ± 93
y-Intercept (model value)	129 ± 3	111 ± 3	129 ± 6	103 ± 4
Slope	0.26 ± 0.01	0.40 ± 0.01	0.22 ± 0.03	0.33 ± 0.02
Mean Bias (model-measured)	−17	−12	−26	−38
Normalized Mean Bias	+2 %	−6 %	−13 %	−11 %
Normalized Mean Error	28 %	25 %	26 %	24 %
RMSE	79	73	89	80
Correlation, R	0.46	0.53	0.49	0.69

Title Page

Abstract | Introduction

Conclusions | References

Tables | Figures

◄◄ | ►►

◄ | ►

Back | Close

Full Screen / Esc

Printer-friendly Version

Interactive Discussion

Table 9. AURAMS $PM_{2.5}$ BC model performance statistics for the 2.5-km grid for the rural Harrow and Bear Creek sites (concentrations in $\mu g\,m^{-3}$).

$PM_{2.5}$BC	Harrow Daytime 09:00–18:00 EST	Harrow Nighttime 18:00–09:00 EST	Bear Creek Daytime 09:00–18:00 EST	Bear Creek Nighttime 18:00–09:00 EST
Number of points	239 (105 min avges) 23 days	139 23 days	295 (3 min avges) 12 days	532 12 days
Model BC Average ± Std Dev	0.16 ± 0.11	0.19 ± 0.12	0.11 ± 0.09	0.15 ± 0.09
Meas BC Average ± Std Dev	0.60 ± 0.28	0.61 ± 0.27	0.38 ± 0.26	0.46 ± 0.32
y-Intercept (model value)	0.070 ± 0.016	0.099 ± 0.02	0.018 ± 0.006	0.090 ± 0.006
Slope	0.15 ± 0.02	0.15 ± 0.04	0.24 ± 0.01	0.14 ± 0.01
Mean Bias (model-meas)	−0.44	−0.42	−0.27	−0.31
Normalized Mean Bias	−73 %	−67 %	−71 %	−67 %
Normalized Mean Error	73 %	69 %	71 %	68 %
RMSE	0.50	0.49	0.34	0.42
Correlation, R	0.39	0.33	0.72	0.46

Evaluation of chemical transport model predictions

C. A. Stroud et al.

Table 10. Detroit-Windsor urban-influenced air masses arriving at Harrow and Bear Creek.

Date (EST)	Model POA HOA NMB RMSE	HOA/OA	Winds	Meteorology	Model BC Meas. BC NMB RMSE	Model CO Meas. CO NMB RMSE	Model SO4 Meas. SO4 NMB RMSE	PMF Source Description
Harrow 21 June, 10:00–15:00	0.28 ± 0.06 1.4 ± 0.4 -81% $1.24\,\mu g\,m^{-3}$	17%	NNW moderate	Winds and PBL heights predicted well	0.15 ± 0.03 0.94 ± 0.17 -84% $0.80\,\mu g\,m^{-3}$	165 ± 15 199 ± 31 -17% $41\,ppbv$	1.86 1.31 42% $0.68\,\mu g\,m^{-3}$	"Organic" factor, South Detroit origin
Bear Creek 8 July, 10:00–14:20	0.32 ± 0.10 0.96 ± 0.23 -67% $0.66\,\mu g\,m^{-3}$	6%	SW moderate	Winds and PBL heights predicted well	0.15 $0.53\ -71\%$ $0.38\,\mu g\,m^{-3}$	194 245 -21% $53\,ppbv$	2.3 13.0 83% $10.6\,\mu g\,m^{-3}$	South Detroit and Windsor origin

Evaluation of chemical transport model predictions

C. A. Stroud et al.

Table 11. Transport from southwest.

Date (EST)	Model POA HOA NMB RMSE	HOA/OA	Winds	Meteorology	Model BC Meas. BC NMB RMSE	Model CO Meas. CO NMB RMSE	Model SO4 Meas. SO4 NMB RMSE	PMF Source Description
Harrow 8 July, 10:00–14:50	0.33 ± 0.12 1.2 ± 0.2 -73 % $0.95 \,\mu g \, m^{-3}$	16 %	SW moderate	Well predicted, evidence for polluted layer aloft	0.16 0.67 -76 % $0.52 \,\mu g \, m^{-3}$	186 248 -25 % 64 ppbv	3.2 5.2 -39 % $2.5 \,\mu g \, m^{-3}$	"Transport" US Midwest
Harrow 27 June, 10:30–14:00	0.47 ± 0.10 0.40 ± 0.14 17 % $0.10 \,\mu g \, m^{-3}$	21 %	SW moderate	Well predicted, evidence for polluted layer aloft	0.16 0.70 -77 % $0.54 \,\mu g \, m^{-3}$	207 231 -11 % 35 ppbv	7.4 4.5 64 % $3.0 \,\mu g \, m^{-3}$	"Transport" US Midwest

Discussion Paper | Discussion Paper | Discussion Paper | Discussion Paper

ACPD

12, 5939–6018, 2012

Evaluation of chemical transport model predictions

C. A. Stroud et al.

Title Page

Abstract | Introduction

Conclusions | References

Tables | Figures

|◄ | ►|

◄ | ►

Back | Close

Full Screen / Esc

Printer-friendly Version

Interactive Discussion

Table 12. Biomass burning influence

Date (EST)	Model POA HOA NMB RMSE	HOA/OA	Winds	Meteorology	Model BC Meas. BC NMB RMSE	Model CO Meas. CO NMB RMSE	Model SO4 Meas. SO4 NMB RMSE	PMF Source Description
Harrow 6 July, 09:00-11:30	0.20 ± 0.04 3.6 ± 0.2 −94 % 3.4 µg m^{-3}	20 %	SE light	Well predicted, switched direction from N to SE	0.15 0.83 -82 % 0.68 µg m^{-3}	201 296 -32 % 104 ppbv	0.59 1.2 −50 % 0.60 µg m^{-3}	"Biomass Burning"
Harrow 7 July, 09:00–14:50	0.48 ± 0.26 1.7 ± 0.3 −71 % 1.22 µg m^{-3}	16 %	WSW moderate	Well predicted, back trajectories originate from NW (Northern Michigan)	0.12 0.82 −86 % 0.70 µg m^{-3}	205 182 13 % 69 ppbv	5.4 1.1 403 % 5.8 µg m^{-3}	"Biomass Burning"

Table 13. Regional Background from the Northwest

Date (EST)	Model POA HOA NMB RMSE	HOA/OA	Winds	Meteorology	Model BC Meas. BC NMB RMSE	Model CO Meas. CO NMB RMSE	Model SO4 Meas. SO4 NMB RMSE	PMF Source Description
Bear Creek 29 June, 12:00–15:00	0.10 ± 0.009 0.13 ± 0.02 -19 % $0.032\,\mu g\,m^{-3}$	5 %	N moderate	Winds predicted well, no plumes	0.042 0.11 -61 % $0.07\,\mu g\,m^{-3}$	130 95 37 % 35 ppbv	0.36 0.51 -30 % $0.12\,\mu g\,m^{-3}$	Not Available
Bear Creek 30 June, 12:30–15	0.17 ± 0.06 0.17 ± 0.05 1 % $0.04\,\mu g\,m^{-3}$	4 %	NE moderate	Winds predicted well, no plumes	0.055 0.17 -69 % $0.14\,\mu g\,m^{-3}$	136 179 -24 % 61 ppbv	2.7 0.99 160 % $1.6\,\mu g\,m^{-3}$	Not Available
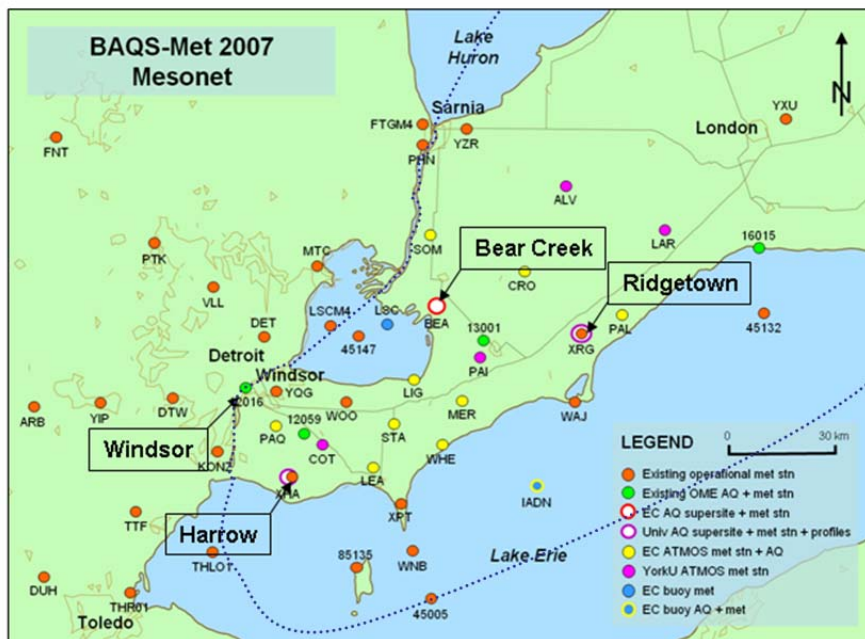
Fig. 1. Locations for the four atmospheric chemistry measurement super-sites (labeled in boxes) in southwestern Ontario, Canada during the BAQS-Met field campaign. Locations for existing and enhanced meteorological stations are also marked. Dotted line represents the US and Canadian border.

Title Page

Abstract | Introduction

Conclusions | References

Tables | Figures

|◄ | ►|

◄ | ►

Back | Close

Full Screen / Esc

Printer-friendly Version

Interactive Discussion
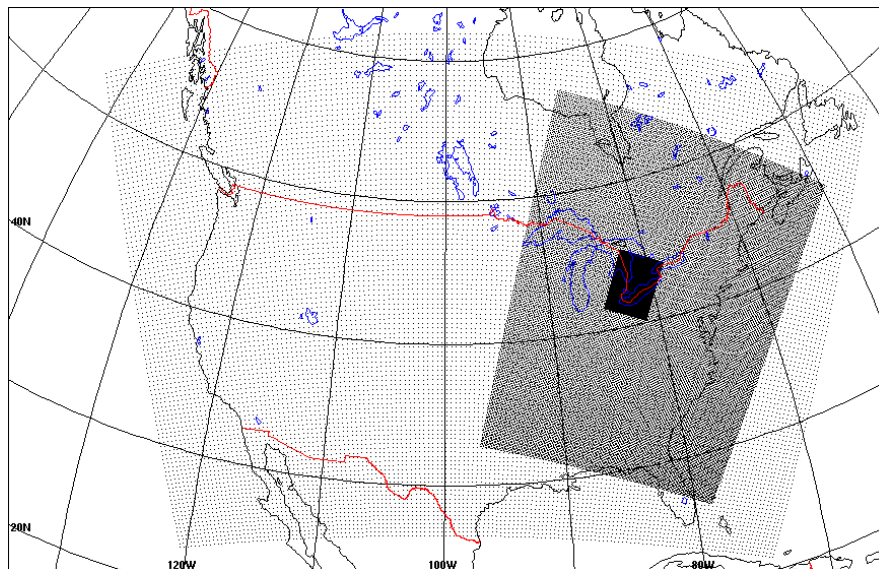
Fig. 2. AURAMS nested grid configuration for BAQS-Met simulations. Outermost grid has a horizontal grid spacing of 42 km. Inner grids have horizontal grid spacings of 15 and 2.5 km, respectively.
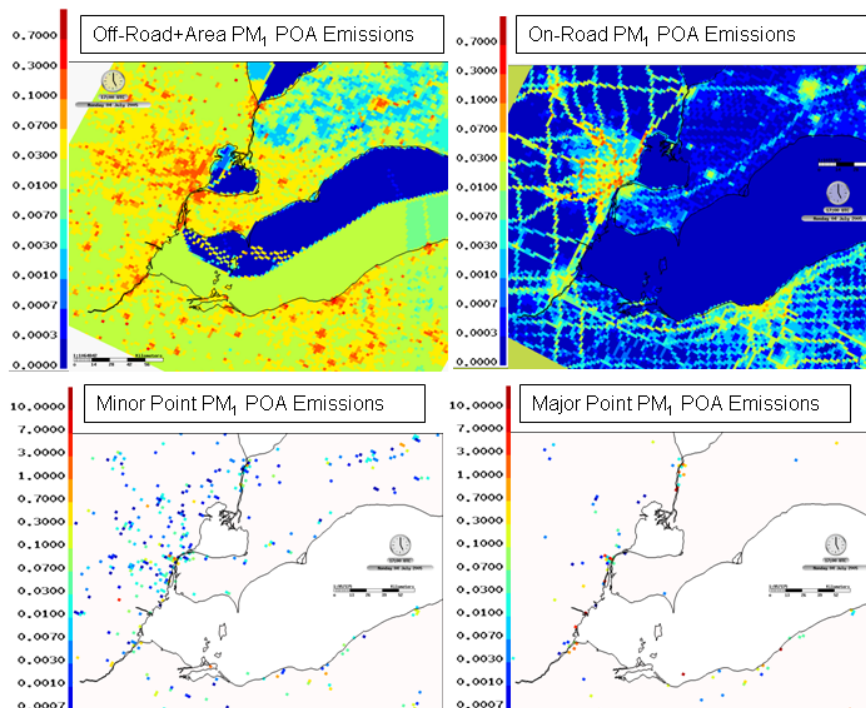
Fig. 3. Example PM$_1$ POA emissions for the 2.5-km innermost domain split into ORAA (upper left), ORM (upper right), minor point (lower left), and major point (lower right) sources on a July, monday at 17:00 UTC (12 EST).

Title Page

Abstract | Introduction

Conclusions | References

Tables | Figures

|◄ | ►|

◄ | ►

Back | Close

Full Screen / Esc

Printer-friendly Version

Interactive Discussion
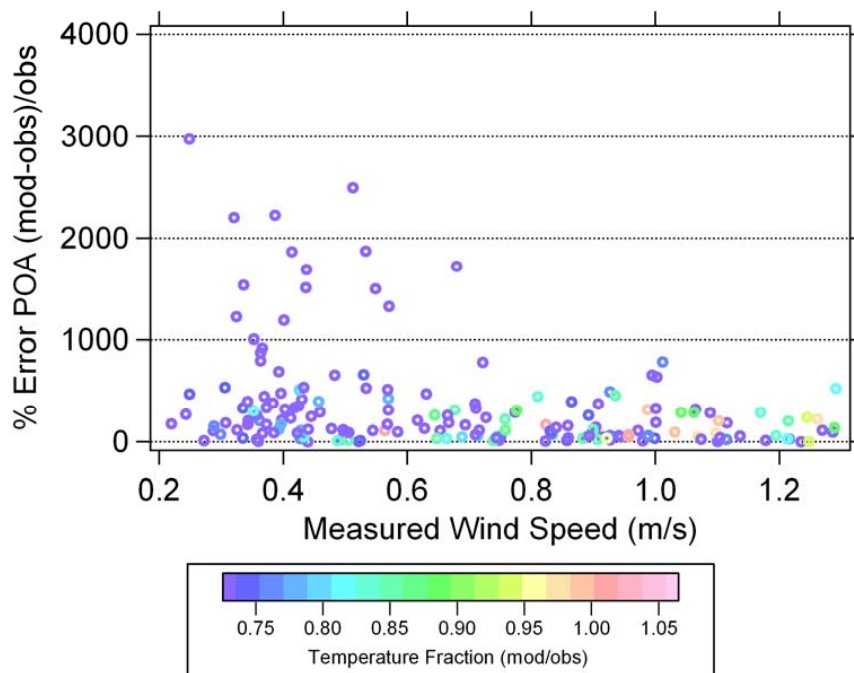
Fig. 4. Model PM$_1$ POA percentage error for nighttime conditions under low winds at Harrow. The colour coding is the ratio of the modeled and measured surface temperature. Under light winds and cooler model surface temperatures, modelled vertical mixing is diminished.
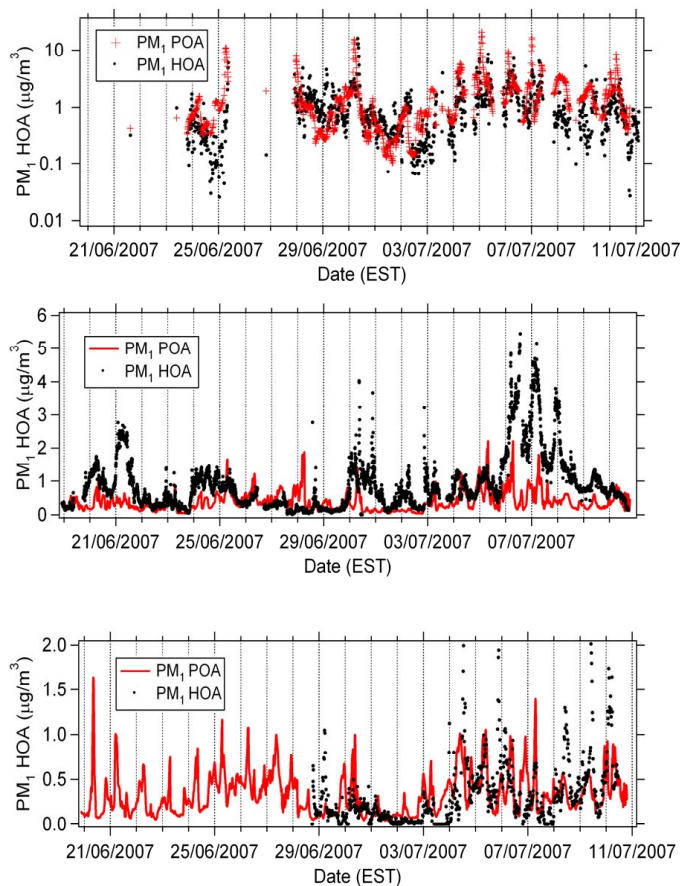
Fig. 5. Time series for HOA plotted with AURAMS PM$_1$ POA at Windsor (top panel), Harrow (middle panel), and Bear Creek (lower panel).
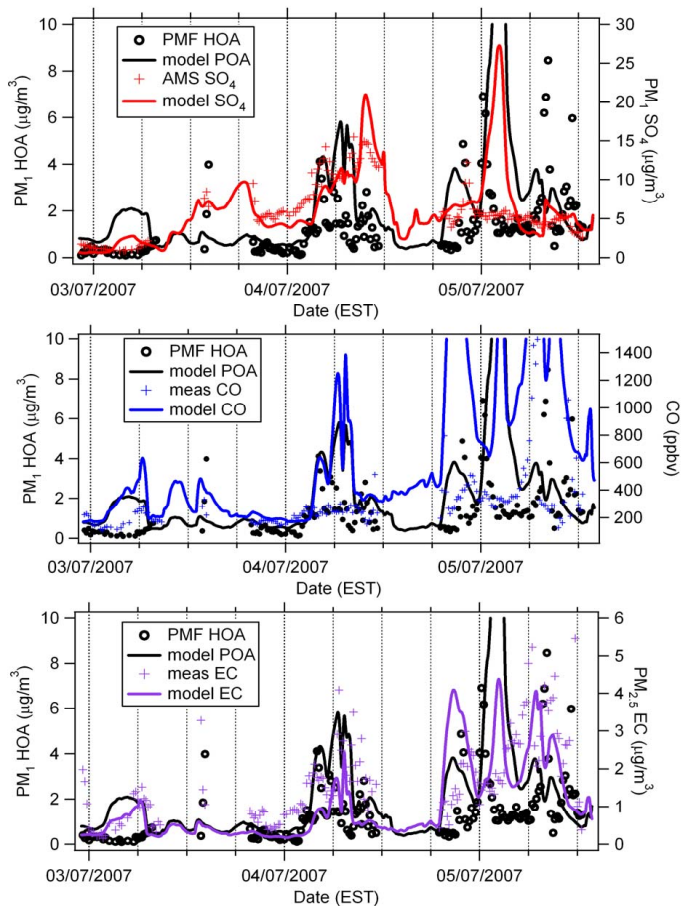
Fig. 6. Selected model PM_1 POA and HOA time series at Windsor from 3 July to 5 July plotted with time series of **(a)** PM_1 SO4, **(b)** CO and **(c)** $PM_{2.5}$ EC measurements and model predictions.

Title Page

Abstract | Introduction

Conclusions | References

Tables | Figures

|◄ | ►|

◄ | ►

Back | Close

Full Screen / Esc

Printer-friendly Version

Interactive Discussion
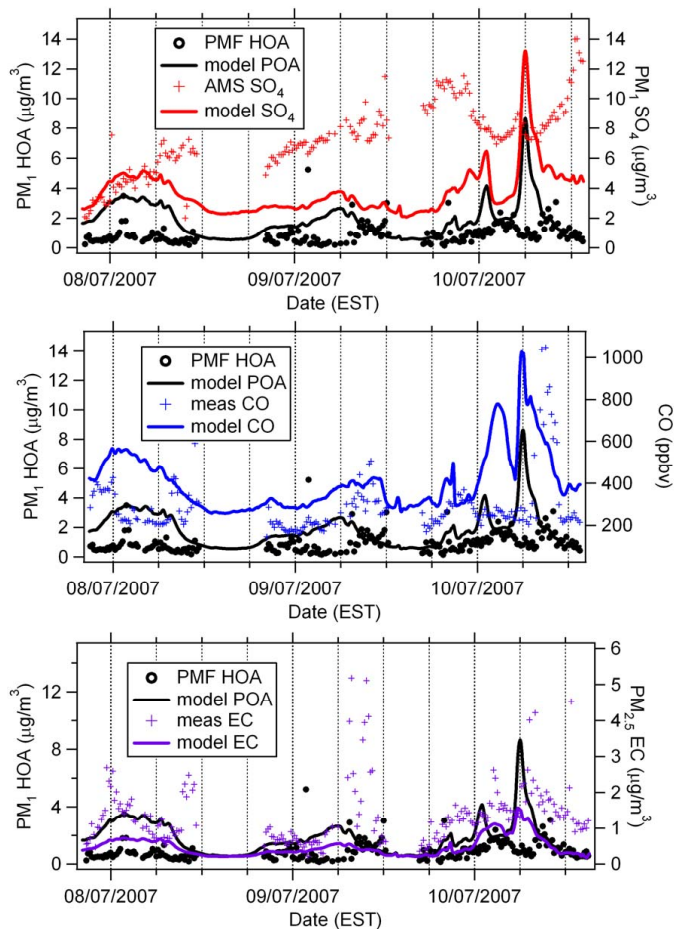
Fig. 7. Same as Fig. 6 but for 8 July to 10 July period.

Title Page

Abstract   Introduction

Conclusions   References

Tables   Figures

◄   ►│

◄   ►

Back   Close

Full Screen / Esc

Printer-friendly Version

Interactive Discussion
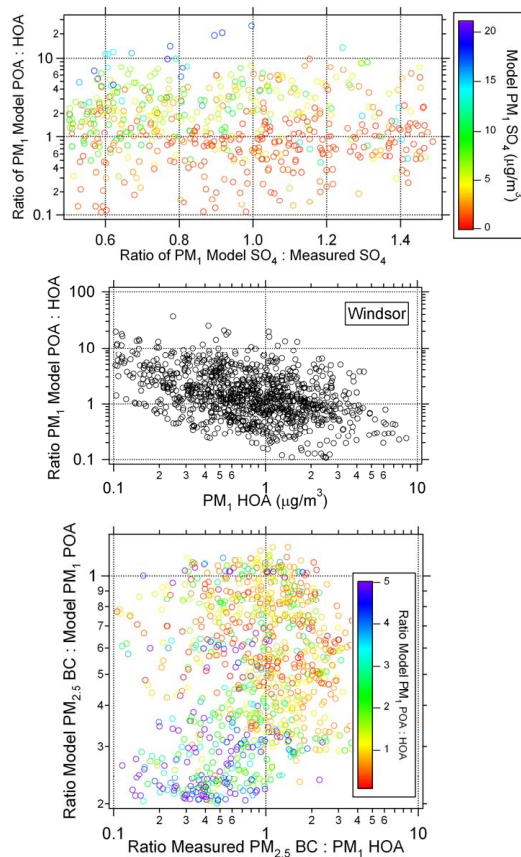
Fig. 8. Scatterplots for Windsor site of **(a)** ratio of PM_1 model POA to HOA vs. ratio of PM_1 model SO_4 to measured SO_4, colour-coded with model SO_4, **(b)** ratio of PM_1 model POA to HOA vs. HOA, and **(c)** ratio of $PM_{2.5}$ model BC to model POA vs. ratio of measured $PM_{2.5}$ BC to HOA, colour-coded with ratio of model POA to HOA (yellow is unbiased, red is HOA underprediction, and blue is HOA overprediction).

Title Page

Abstract | Introduction

Conclusions | References

Tables | Figures

◄ | ►|

◄ | ►

Back | Close

Full Screen / Esc

Printer-friendly Version

Interactive Discussion
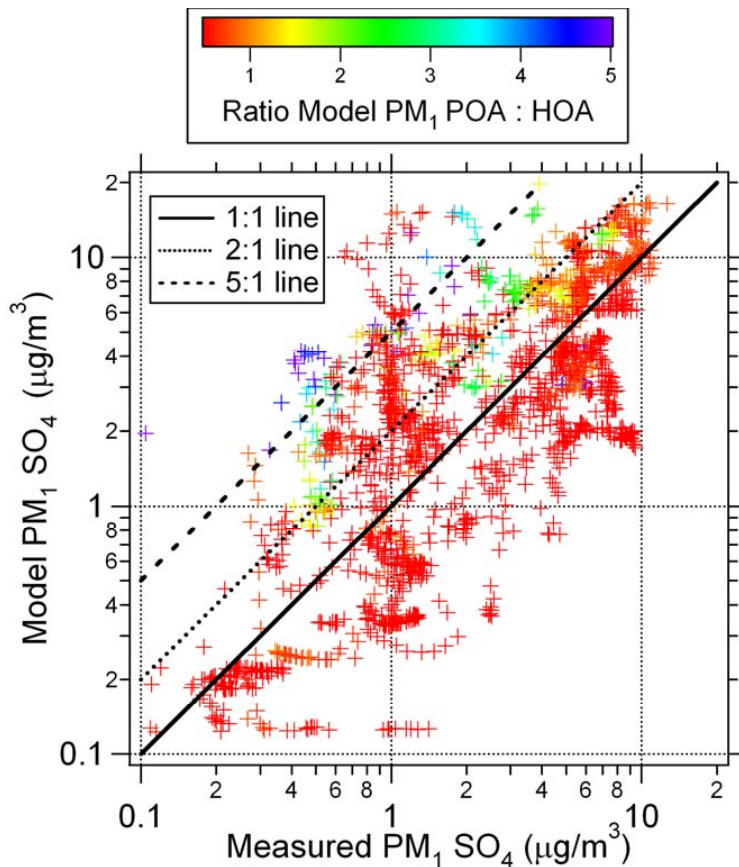
Fig. 9. Correlation of modeled SO$_4$ and measured SO$_4$ at Harrow, coloured-coded as a function of the ratio of model POA to HOA, for the period from 19 June to 10 July 2007.
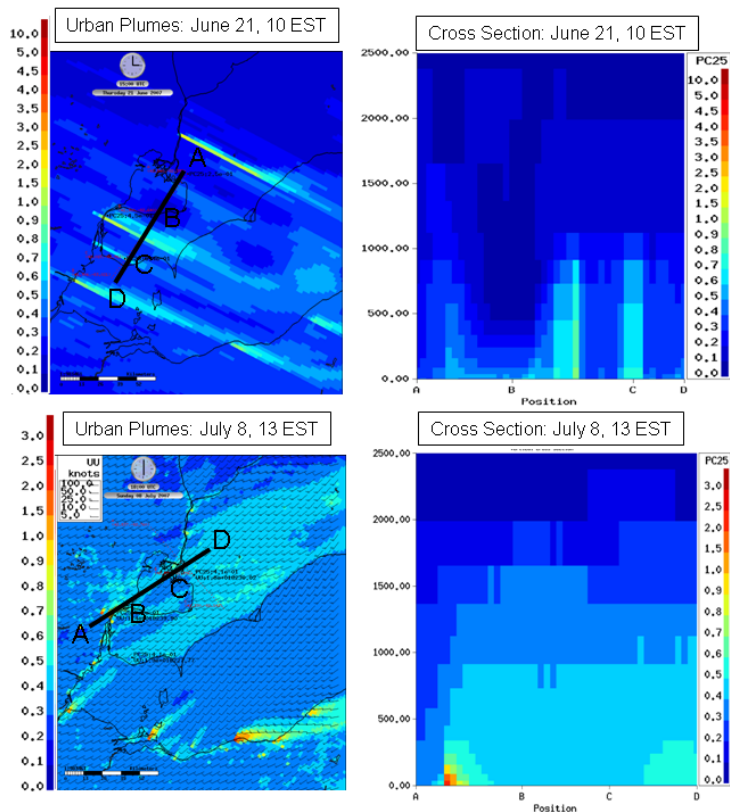
Fig. 10. AURAMS **(a)** POA distribution for 21 June 2007 at 10:00 EST (upper left) and **(b)** vertical cross section perpendicular to surface wind direction at Harrow from point A in northeast to point D in southwest (upper right), **(c)** POA distribution with superimposed surface wind vectors for 8 July 2007 at 13:00 EST at Bear Creek (lower left) and **(d)** vertical cross section parallel to surface wind direction from point A in southwest to point D in northeast (lower right).

Title Page

Abstract | Introduction

Conclusions | References

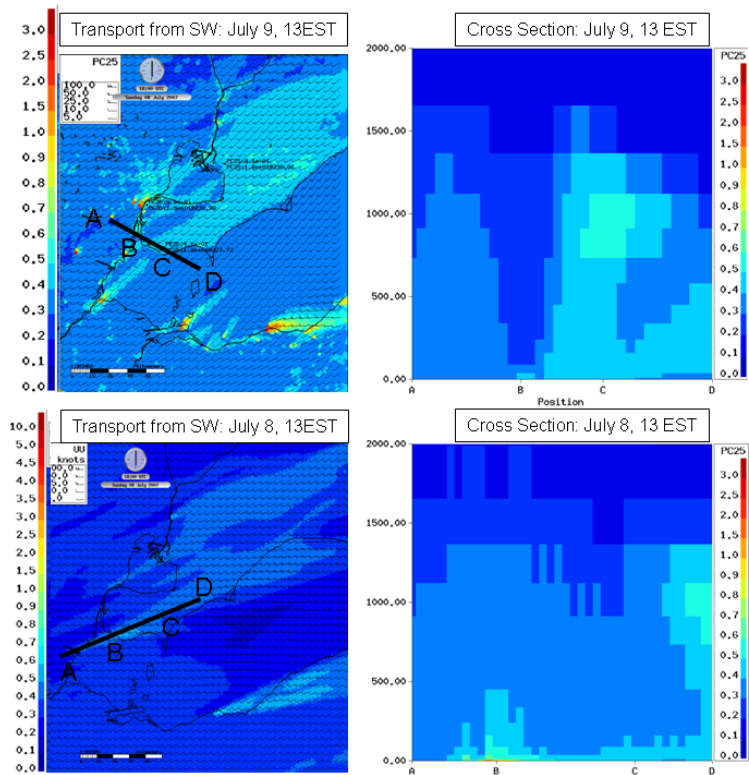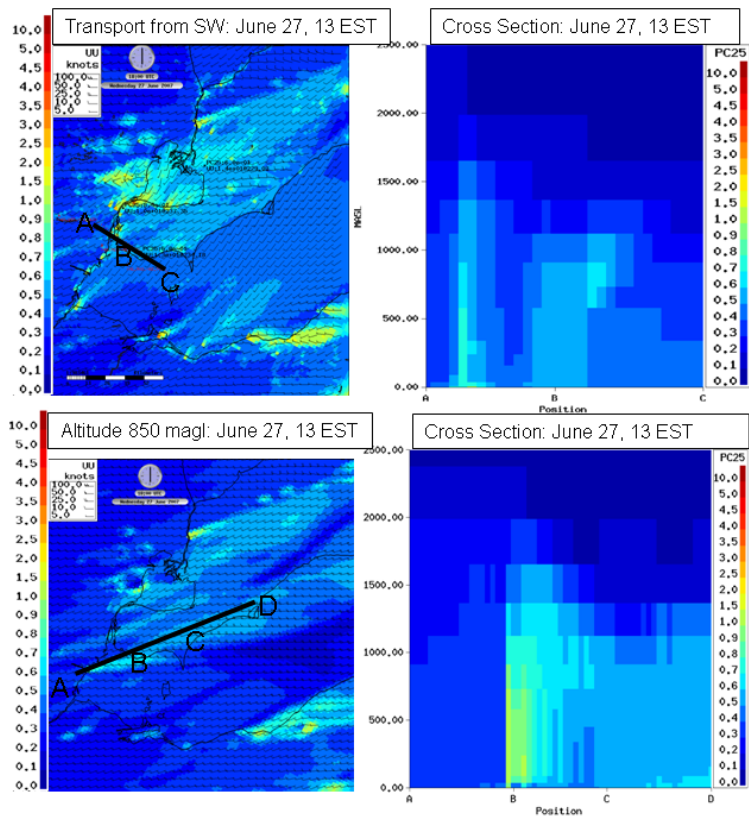Tables | Figures

◀◀ | ▶▶

◀ | ▶

Back | Close

Full Screen / Esc

Printer-friendly Version

Interactive Discussion

Fig. 11. AURAMS **(a)** POA distribution with superimposed surface wind vectors for 8 July 2007 at 13:00 EST (upper left) and **(b)** vertical cross section perpendicular to surface wind direction at Harrow from point A in northwest to point D in southeast (upper right), **(c)** POA distribution at 815 m a.s.l. with superimposed surface wind vectors for 8 July 2007 at 13:00 EST (lower left) and **(d)** vertical cross section parallel to wind direction at Harrow from point A in southwest to point D in northeast (lower right).

Title Page

Abstract | Introduction

Conclusions | References

Tables | Figures

◄◄ | ►►

◄ | ►

Back | Close

Full Screen / Esc

Printer-friendly Version

Interactive Discussion

Fig. 12. AURAMS **(a)** POA surface distribution with superimposed surface wind vectors for 27 June 2007 at 13:00 EST and **(b)** vertical cross section perpendicular to surface wind direction at Harrow from point A in northwest to point C in southeast, **(c)** POA distribution at 815m with superimposed surface wind vectors for 27 June 2007 at 13:00 EST and **(d)** vertical cross section parallel to surface wind direction at Harrow from point A in southwest to point D in northeast.